Author Version of : Science of The Total Environment, vol.827; 2022; Article no: 154260

Unraveling the sources of atmospheric organic aerosols over the Arabian Sea: insights from the stable carbon and nitrogen isotopic composition

Poonam Bikkina[1,*], Srinivas Bikkina[1,2], Kimitaka Kawamura[2], V.V.S.S. Sarma[3], Dhananjay K. Deshmukh[2]

[1]CSIR-National Institute of Oceanography, Dona Paula, Goa 403 004, India

[2]Chubu Institute of Advanced Sciences, Chubu University, Kasugai-shi, Aichi, 4878501, Japan

[3]CSIR-National Institute of Oceanography, Regional Cente Waltair, Visakhapatnam 530017, India

*Corresponding author :Dr. Poonam Bikkina (ptyagi@nio.org)

Abstract

The isotopic compositions of stable carbon ($\delta^{13}C$) and nitrogen ($\delta^{15}N$) in marine aerosols influenced by the continental outflows are useful proxies for understanding the aging and secondary formation processes. Every winter, the haze pollutants transported from South Asia significantly affect the chemical composition of marine atmospheric boundary layer of the Arabian Sea. Here, we assessed the $\delta^{13}C$ of total carbon (TC) and $\delta^{15}N$ of total nitrogen (TN) in marine aerosols collected over the Arabian Sea during a winter cruise (6-24 December 2018). TC (2.1-13.4 µg m^{-3}) is strongly correlated with TN (0.9-5.0 µg m^{-3}), likely because of their common source-emissions, biomass burning and fossil-fuel combustion in the Indo-Gangetic Plain and South Asia (corroborated by backward-air mass trajectories and satellite fire counts). Besides, the linear relationship between the mass ratios of water-soluble organic carbon (WSOC) to TC (0.04-0.65) and $\delta^{13}C_{TC}$ (-25.1‰ to -22.9‰) underscores the importance of aging process. This means oxidation of organic aerosols during transport not only influences the WSOC levels but also affects their $\delta^{13}C_{TC}$. Likewise, the prevalent inverse linear relationship between the equivalent mass ratio of (NH_4^+ /non-sea-salt- or nss-SO_4^{2-}) and $\delta^{15}N_{TN}$ (+15.3‰ to +25.1‰) emphasizes the overall significance of neutralization reactions between major acidic ([nss-SO_4^{2-}] >>[NO_3^-]) and alkaline species (NH_4^+) in aerosols. Higher $\delta^{15}N_{TN}$ values in winter than the spring inter-monsoon clearly emphasizes the significance of the anthropogenic combustion sources (i.e., biomass burning) in the South Asian outflow. A comparison of $\delta^{13}C_{TC}$ and $\delta^{15}N_{TN}$ with the source emissions revealed that crop-residue burning emissions followed by the coal fired power plants mostly dictate the atmospheric abundance of organic aerosols in the wider South Asian outflow.

Keywords: Organic aerosols, stable carbon and nitrogen isotopic composition, Arabian Sea, continental outflow, aging effect.

Graphical Abstract

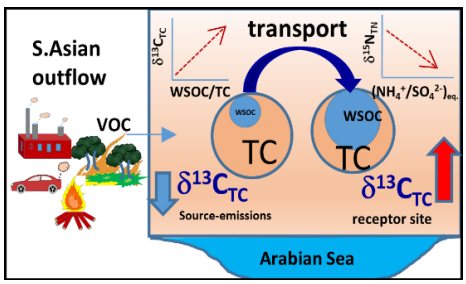

1. Introduction

Organic aerosols (OA), a major component of atmospheric particulate matter, influence regional and global climate via the direct (*i.e.,* scattering/absorption) and/or indirect effects (*e.g.* hygroscopicity, cloud condensation nuclei) (Jacobson et al., 2000; Kanakidou et al., 2005; Fuzzi et al., 2006). The major sources of OA over the continents include biomass burning/biogenic emissions and fossil-fuel combustion(Gustafsson et al., 2009; Bosch et al., 2014; Bikkina et al., 2017a). Apart from the direct emissions, secondary formation processes involving the condensation of semivolatile organic compounds (SVOC) also contribute to OA abundances(Kroll and Seinfeld, 2008; Jimenez et al., 2009). It is, therefore, important to understand the evolving characteristics of OA during long-range transport to accurately predict their overall effect on atmospheric radiative forcing (Fuzzi et al., 2006; Jimenez et al., 2009). Towards this, modeling studies seek to incorporate the major factors affecting the abundances of OA during transport (Huebert and Charlson, 2000). Therefore, a better parameterization and inclusion of any such factor in the climate model would improve our existing understanding of the radiative effects of cloud/aerosol interactions(Li et al., 2016).

Probing the influential factors of atmospheric OA over continental sites is more complicated because of the inadvertent contribution, mixing from direct emissions and secondary formation processes. Alternatively, the coastal oceans that are downwind of continental pollution sources serve as an ideal choice for assessing the controlling factors of atmospheric abundance of OA during their transit to remote locations (Chesselet et al., 1981; Cachier et al., 1986; Kawamura et al., 2004; Kirillova et al., 2013; Xiao et al., 2018; Zheng et al., 2018; Bikkina et al., 2019a; Elliott et al., 2019). However, it is important to note that organic matter associated with nascent sea-spray emissions also contributes to marine aerosols. To circumvent this problem, one needs to use a tracer that is influenced by the ageng processes (*i.e.,* either oxidation or secondary formation processes) and also at the same time can help us in distinguishing the relative influence of continental versus marine emissions.

Stable carbon and nitrogen isotopic compositions ($\delta^{13}C_{TC}$ and $\delta^{15}N_{TN}$, respectively) of total carbon (TC) and nitrogen (TN) in atmospheric aerosols have proven useful to understand the sources and processes affecting the chemical composition (Kundu et al., 2010a; Pavuluri and Kawamura, 2012; Kirillova et al., 2013; Aguilera and Whigham, 2018; Bikkina et al., 2019b; Bikkina et al., 2020b; Morera-Gómez et al., 2021). Studies have shown that airborne particulate organic matter emitted along with sea-spray has a characteristic higher $\delta^{13}C_{TC}$ values (−21±2‰)(Chesselet et al., 1981; Cachier et al., 1986; Miyazaki et al., 2011) and differ from that of continental origins (burning

of C_3 plants: –25‰ to –32‰; burning of C_4 plants: −13.5‰ to −11.5‰, coal combustion: −25‰ to −21‰, vehicular emissions: −28‰ to −26‰)(Cachier et al., 1986; Turekian et al., 1998; Martinelli et al., 2002; Widory, 2006; Cao et al., 2011). Considering the disparity between source-emissions, the $\delta^{13}C_{TC}$ and $\delta^{15}N_{TN}$ in marine aerosols influenced by the continental outflows would provide insights on transformations of OA during atmospheric transport (Cachier et al., 1986; Bikkina et al., 2016b).

During atmospheric transport, several factors such as oxidation and secondary organic aerosol formation influence the abundance/composition of aerosols over the marine region. Towards this, the interrelationships between stable isotopic composition of C and N isotopic composition of marine aerosols are useful for better constraining the relative significance of these factors (Pavuluri et al., 2010; Bikkina et al., 2016b; Rastogi et al., 2020; Singh et al., 2021b). In winter season, the surface waters of the eastern Arabian Sea is highly productive because of the convective mixing (Madhupratap et al., 1996; Kumar et al., 2001) and is also influenced by the long-range atmospheric transport of pollutants in the Indo-Gangetic Plain (IGP) and southern India (Kumar et al., 2008a; Bikkina et al., 2012; Aswini et al., 2020). The present study focusses on the influence of various source emissions (oceanic vs. continental) and processing effects of OAs in the South Asian outflow to the coastal and offshore waters of the eastern Arabian Sea during a winter cruise (SS379: 6-24 December 2018). Here, we measured the concentrations of total carbon (TC) and total nitrogen (TN) along with their stable carbon and nitrogen isotopic compositions ($\delta^{13}C_{TC}$ and $\delta^{15}N_{TN}$, respectively). We used other chemical composition data including water-soluble inorganic ions, methanesulfonic acid, and carbonaceous components to substantiate the arguments related to sources and formation pathways of OA.

2. Materials and methods

2.1. Analysis of stable carbon and nitrogen isotopic composition

Seventeen TSP samples were collected using a high-volume air sampler (Envirotech Pvt. Ltd.; flow rate: 1.0 $m^3\,min^{-1}$), which was set up onboard FORV Sagar Sampada (SS379), conducted in the offshore waters of the Arabian Sea, started at Kochi on 6 December 2018 and ended at Okha port in Gujarat on 25 December 2018 (Bikkina et al., 2021). The TSP sampler was set at the edge in front of Ship's navigation room at a height of ~10 m above sea level. We operated the air sampler only when the ship is cruising at a speed of 10 knots/ hour and winds blow from the bow side to avoid any contamination from the ship's exhaust. All samples were collected on Tissuquartz filters (PALLFLEX®™, 8"× 10"), which were wrapped in aluminium foils and precombusted at 450 °C for

6 h. These filters were placed in airtight Ziploc bags and subsequently stored at -20 °C until analysis. For more details regarding aerosol collection, prevailing meteorology and other chemical composition data, reference is made to Bikkina et al. (2020a).

We measured the mass concentrations of TC and TN along with $\delta^{13}C_{TC}$ and $\delta^{15}N_{TN}$ using an elemental analyzer coupled to an isotope ratio mass spectrometer (EA/irMS, model: Carlo Erba NA 1500 EA + Finnigan MAT Delta plus). All the tin cups were precleaned with acetone prior to their use, and dried overnight in our laboratory. Approximately 20 mm diameter filter punches were wrapped in tin cups and introduced into the first quartz combustion column filled with chromium oxide (Cr_2O_3) and Co_3O_4+Ag (*i.e.*,for scrubbing sulphur and halogenated gases) and heated to 1020 ºC. In this first column, TC and TN from a sample were converted to CO_2 and NO_x, respectively. These gases were then introduced into the second reduction column of the EA containing Cu fillings and, the NO_x is reduced to molecular N_2 by passing through a reduction column containing Cu filings. Both CO_2 and N_2 gases were separated on a gas chromatograph and then introduced to the irMS through an interface (ConFlo II) for the measurement of $\delta^{13}C_{TC}$ and $\delta^{15}N_{TN}$. The stable isotopic composition is often expressed as the relative deviation of heavier to lighter isotope ratio in a sample to that of standard, Pee Dee Belemnite (PDB) for TC and atmospheric N_2 for TN using the method detailed in Kawamura et al. (2004).

$$\delta^{13}C = \left[\frac{\left({}^{13}C/_{12}C\right)_{sample}}{\left({}^{13}C/_{12}C\right)_{std}} - 1\right] \times 1000 \quad (1)$$

$$\delta^{15}N = \left[\frac{\left({}^{15}N/_{14}N\right)_{sample}}{\left({}^{15}N/_{14}N\right)_{std}} - 1\right] \times 1000 \quad (2)$$

2.2. Quality assurance

Before measuring the samples for $\delta^{13}C_{TC}$ and $\delta^{15}N_{TN}$, we have calibrated the EA-irMS with a five-point calibration using a known isotopic composition of acetanilide standard for assessing the TC and TN content in marine aerosols from the Arabian Sea (Kawamura et al., 2004; Bikkina et al., 2016b). The analytical uncertainties associated with the $\delta^{13}C_{TC}$ and $\delta^{15}N_{TN}$ from this study are within 0.2 and 0.5‰, respectively. We also analyzed tin cups for blanks and procedural lab and field blanks prior to the TSP samples on the EA-irMS. The carbon and nitrogen content in field blanks were only

~0.5% of the average analytical signal obtained for the aerosol samples. The $\delta^{13}C_{TC}$ and $\delta^{15}N_{TN}$ were then corrected for blanks based on the mass balance approach as detailed in Kawamura et al. (2004).

A portion of aqueous extract of the TSP sample was passed through a 0.22 µm syringe filter (PVDF, Milex-GV) and measured for anions *(e.g.,* MSA, Cl^-, NO_3^-, and SO_4^{2-}) and cations (Na^+, NH_4^+, K^+, Ca^{2+} and Mg^{2+}) using the ion chromatography (Bikkina et al., 2021). Likewise, another portion of filtered aqueous extract was analyzed for water-soluble organic carbon (WSOC) on the Shimadzu total carbon analyzer (TOC). More explicit details about the analytical protocols and quality assurance details for the SS259 cruise were detailed elsewhere (Bikkina et al., 2020a; Bikkina et al., 2021). These pararmeters were only used to support the inferences related to the sources and processing effects of OA during transport from South Asia.

3. Results and discussion

3.1. Backward air mass trajectories and MODIS fire counts

Backward air mass trajectories (BTs) are proven as a powerful tool to trace the likely continental source regions affecting the composition of ambient TSP (Draxler, 2002) and, hence, the TC and TN aerosols during the SSD079 cruise. Therefore, we computed seven-day isentropic BTs using the archived meteorological datasets of National Center for Environmental Prediction and National Center for Atmospheric Research (NCAR) reanalysis in the hybrid single particle Lagrangian integrated trajectory model (HYSPLIT, version-4;(Stein et al., 2015)). Numerous studies have shown that biomass burning over South Asia is a prominent source of organic aerosols over the tropical Indian Ocean during winter season (Lelieveld et al., 2001; Guazzotti et al., 2003; Gustafsson et al., 2009). Consequently, we examined the fire count data from the satellite retrievals of Moderate Resolution Imaging Spectroradiometer (MODIS) over South Asia during the study period (December 2018) to understand the impact of postharvest crop-residue burning emissions on the atmospheric abundances and the stable carbon and nitrogen isotopic composition of TC and TN aerosols, respectively over the Arabian Sea (Table 1).

3.2. Spatial variability of TC and TN concentrations

When we combined the BT paths corresponding to the sampling dates of TSP from this study with the MODIS fire count data over South Asia, it is evident that open burning practices of crop residues in the northwestern IGP and southern India significantly influenced the atmospheric TC and TN aerosols during the SS379 cruise (Figure 1). Accordingly, we observed significant temporal variability in the mass concentration of TC (2.1-13.4 µg m^{-3}; av. 7.2±3.4 µg m^{-3}) and TN (0.9-5.0 µg m^{-3};av.2.8±1.2 µg m^{-3}), respectively. The TC measured on EA (this study) was in good agreement

with the sum of mass concentrations of organic carbon (OC) and elemental carbon (EC) independently measured on a Sunset Lab carbon analyzer ((Bikkina et al., 2020a); Figure 2a). This consistency further validates the reliability of $\delta^{13}C_{TC}$ values from this study. Besides, TN loadings strongly correlated with TC over the Arabian Sea, suggesting their similar source emissions and/or their common atmospheric long-range transport history (Figure 2b). This argument is further supported by the observed similar spatial variability of TC, TN and TC/TN ratios over the Arabian Sea with somewhat high concentrations reported over the northern latitudes (Figure 3a-c). The TC/TN ratios in marine aerosols decreased from north to south (Figure 3c), possibly due to a prominent influence of pollution sources in the IGP. This inference was further supported by the backward air mass trajectories and MODIS-satellite based fire counts originated from the biomass burning source regions in the northwestern IGP (Figure 2). TC and TN loadings over the Arabian Sea are comparable to those reported from other continentally influenced marine regions (the Bay of Bengal, Arabian Sea, East China Sea, South China Sea), but higher than those from the remote oceans (Table 2; the western North Pacific, Arctic Ocean, Antarctic Ocean)(Chesselet et al., 1981; Cachier et al., 1986; Kawamura et al., 2004; Miyazaki et al., 2011). However, TC and TN concentrations from our winter cruise in the Arabian Sea are lower than those reported from the several continental urban/rural sites in India (Table 2).

3.3. Spatial variability of $\delta^{13}C_{TC}$

The $\delta^{13}C_{TC}$ of TSP samples collected over the Arabian Sea varied from -25.1‰ to -22.9‰ (-24.0±0.7‰; Figure 4a). These values are significantly lower than those documented for the airborne particulate organic matter from the remote oceans (−21±2‰)(Chesselet et al., 1981; Cachier et al., 1986; Miyazaki et al., 2011). This results suggests that the the source-emissions from South Asia significantly influence the measured $\delta^{13}C_{TC}$ signatures over the Arabian Sea during the winter cruise. Atmospheric mineral dust is a significant contributor to ambient TSP samples in the continental outflows to the tropical Indian Ocean (Rastogi and Sarin, 2006; Bikkina et al., 2014). In particular, the dust particles in the winter season are typically comprised of the fine alluvium of the IGP, whereas those from the spring-intermonsoon season (March-May) are mostly enriched in coarse particles, originating from Thar and other deserts in the Middle East (Bikkina and Sarin, 2012). Given the impact of IGP-outflow on the Arabian Sea during SS379 cruise, which is corroborated by the backward airmass trajectories, we presumed that the mineral dust is mostly sourced from the IGP.

The soils of the IGP are significantly affected by the carbonate weathering of the major rivers such as the Ganga,Yamuna, Brahmaputra, Gaghra and the Gandak (Sarin et al., 1989; Krishnaswami and Singh, 1998). This process is in turn often held responsible for the abundance of Ca, Mg, HCO_3^- and CO_3^- in these major river systems (Sarin et al., 1992). As a consequence, the fine alluvial bed sediment in the IGP, an important source of mineral dust during winter season, is depleted in carbonates (Bikkina et al., 2014). Besides, the carbonates of mineral dust are, in general, characterized by the $\delta^{13}C$ values close to zero permil (-1.2‰ to 1.3‰; -3‰ to -6‰; (Achyuthan et al., 2007; Cao et al., 2008; Chen et al., 2015)). As such the abundance of carbonate fraction in the TSP samples often causes a slight enrichment of ^{13}C of TC compared to those from the mixture of anthropogenic/biogenic sources (−30‰ to −23‰) (Bikkina et al., 2016b; Rastogi et al., 2020). In our samples, the mass balance approach has revealed that mineral dust accounts for ~55±10% of TSP mass concentration over the Arabian Sea (Bikkina et al., 2020a). This is based on the remaining unaccounted fraction of TSP load after subtracting the contribution of anthropogenic water-soluble inorganic species (nss-SO_4^{2-}+NO_3^-+NH_4^++nss-K^+: 20.9±8.8%), sea salt (14.6±5.8%), particulate organic matter (21.4±10.1%) and elemental carbon (2.3±1.1%)(Bikkina et al., 2020a).

Despite such high abundance of dust over the Arabian Sea (~50%), we could not observe any significant difference in the $\delta^{13}C_{TC}$ before and after exposing the SS379 aerosol filters to HCl fumes. Previous studies have documented that the fine alluvium of IGP is characterized by a much lower $\delta^{13}C$ values (Agnihotri et al., 2011a; Sharma et al., 2015; Singh et al., 2018; Singh et al., 2021a) than the carbonate rich coarser mineral dust from the Thar Desert (Agnihotri et al., 2020). Therefore, if carbonates remained as a major fraction of the atmospheric dust sampled over the Arabian Sea, then we could expect a remarkable difference in $\delta^{13}C_{TC}$ before and after acid treatment. Since the differences in $\delta^{13}C_{TC}$ between before and after acid treatment are rather small in our cruise samples, it is therefore implicit that carbonate fraction is not a major component of wintertime dust over the Arabian Sea. Agnihotri et al. (2015) exposed the ambient aerosols collected over Goa, a coastal city in the southern India and also close to our cruise track, from winter and summer seasons to HCl fumes and measured the $\delta^{13}C$ before and after acid-treatment. In their study, the summertime TSP showed some discrepancy in $\delta^{13}C$ before (-24.9±1.3‰) and after HCl fumigation (-26.4±0.4‰) because of the influence of carbonate rich dust from Thar Desert in Rajasthan (Agnihotri et al., 2015). In contrast, Agnihotri et al. (2015) could not detect such difference in $\delta^{13}C$ between before and after HCl-treated aerosols from winter season ($\delta^{13}C_{TC}$: -24.9±0.8‰; and $\delta^{13}C_{TOC}$: -24.8±0.4‰). This result from Agnihotri et al. (2015) is somewhat consistent with our findings from the winter cruise data in the Arabian Sea, which is mainly due to the impact of long-range transport of fine

alluvium and anthropogenic emissions in the IGP. Overall, it is evident from Figure 4a that the heavier isotopes of TC (northern latitudes) are probably due to the influence of atmospheric aging of ambient organic aerosols from the South Asian outflow in addition to the contribution from anthropogenic/biogenic sources.

3.4. Spatial variability of $\delta^{15}N_{TN}$

The $\delta^{15}N_{TN}$ in marine aerosols collected over the Arabian Sea during the winter cruise varied from +15.3‰ to 25.1‰ with an average of +19.5±2.1‰ (Figure 4b). Here, the range of $\delta^{15}N_{TN}$ values is comparable to those previously observed over the Bay of Bengal for the wintertime aerosols during the impact of continental outflow from the IGP (+20.4±5.4‰) and southeast Asia (+19.4±6.1‰) (Bikkina et al., 2016b). On the other hand, our $\delta^{15}N_{TN}$ values from this study are much higher than those documented for the spring-intermonsoon cruises in the Arabian Sea (-2.3‰ to +12.7‰;) and the Bay of Bengal (+5.6‰ to +15.2‰)(Agnihotri et al., 2011a)). Besides, the $\delta^{15}N_{TN}$ values over the Arabian Sea showed remarkable consistency with the biomass burning emissions (range: +15.8 to +25.1‰; av. +19.4±2.1‰) sampled over Southeast Asia (Boreddy et al., 2018) but somewhat lower compared to those observed for Amazonian forest fires (+23.5‰ to +25.7‰; av. +23.5‰) (Kundu et al., 2010a). Furthermore, the Arabian Sea samples are more enriched with ^{15}N compared to those typically observed for the emissions from diesel/gasoline-based vehicles (+4.6±0.6‰;(Widory, 2007)) and coal fired power plants (+6 to +18‰(Heaton, 1990)).

Vehicular emissions primarily based on diesel and gasoline combustion contribute to lower values of $\delta^{15}N_{TN}$ (<0‰) compared to those originating from coal-fired power plants (9‰)(Heaton, 1990; Widory, 2007). The high temperatures (>2000 °C) caused by the spark ignition in the internal combustion engines of diesel/gasoline-fueled vehicles facilitate the reaction of atmospheric N_2 ($\delta^{15}N$ = +0‰) with O_2 (*i.e.,* $N_2 + O_2 \rightarrow 2NO$). However, this process introduces a kinetic isotope effect (KIE) in which lighter N-containing isotopologues react preferentially with O_2 to yield NO containing less $\delta^{15}N$ (–2‰(Heaton, 1990); –1.8‰). Coal contains a substantial amount of organic nitrogen. Also, coal combustion in the thermal-fired power plants is relatively a low temperature process (1300-1400 °C) than that occur in the internal combustion engines of automobiles. It is important to reiterate that NO_x emissions from the coal power plants result from thermal breakdown of organic matter of the fuels, which is unlike those emissions from vehicular exhaust (i.e., generated from the compressed air)(Widory, 2007). As a result, NO_x from the coal fired power plants are relatively enriched in ^{15}N ($\delta^{15}N$:+1‰ to +5‰) (Feng et al., 2020) compared to that of atmospheric N_2 ($\delta^{15}N$: +1.0‰ to +1.2‰)(Heaton, 1990). Heaton (1990) ascribed this enrichment to the substantial

decrease in the NO_x concentrations by the reaction with nitrogen radicals to yield molecular nitrogen, which introduces KIE and, hence, leftover NO is enriched in ^{15}N.

Although Arabian Sea is witnessing the impact South Asian outflow in winter, which is similar to that of influence of pollution sources in East Asia over the East China Sea and Western North Pacific (WNP), there exist some striking differences with regard to relative abundances of inorganic versus organic aerosol-N fractions. Over South Asia, the radiocarbon based source apportionment of organic aerosols revealed that 80% contribution from biomass burning/biogenic emissions(Gustafsson et al., 2009; Sheesley et al., 2012; Bosch et al., 2014; Kirillova et al., 2014b; Bikkina et al., 2016a). As a consequence, relatively high emissions of NH_3 and organic nitrogen (for e.g., urea, a fertilizer) from the crop-fields during harvesting period as well as emissions from animal livestock husbandry mostly contribute to concordant rise in the atmospheric levels of NH_4^+ and organic nitrogen in the South Asian outflow. This is in accordance with the prevailing high concentrations of particulate NH_4^+ and organic nitrogen over the Arabian Sea and the Bay of Bengal in winter season (Agnihotri et al., 2011a; Bikkina et al., 2011; Rastogi et al., 2020; Bikkina et al., 2021). Unlike South Asia, the ^{14}C-based source apportionment of atmospheric particulate organic matter and other chemical components over East Asia revealed major footprints from fossil-fuel combustion, i.e., coal fired thermal power plants and vehicular exhaust emissions (Kirillova et al., 2014a; Zhang et al., 2014; Andersson et al., 2015; Zhang et al., 2015; Fang et al., 2018). Recent top down estimates of NO_x emissions over East Asia indicated that the fossil-fuel combustion sources mostly contribute to NO_3^- along with a minor contribution of NH_4^+ and organic N (Pani et al., 2017; Qu et al., 2022). These inferences were further corroborated by other studies based on $\delta^{15}N$ of bulk and individual nitrogen components (Kundu et al., 2010b; Park et al., 2018). Apart from the differences in the source-emissions of aerosol-N between both the continental outflows, however, there is also a regional variability of ambient temperature and relative humidity (RH) levels between South Asia and East Asia that could affect the relative abundances of major aerosol-N species and hence, reflected in the $\delta^{15}N_{TN}$.

3.5. Quantitative estimation of continental TC

The $\delta^{13}C_{TC}$ of particulate organic matter in the remote marine aerosols is distinctly different from those of the continentally derived ones (Chesselet et al., 1981). Therefore, we can constrain the relative proportions of continentally derived TC using a two endmember mixing model between marine biogenic and continental organic aerosols. Based on the approach suggested by the Chesselet

et al. (1981), the $\delta^{13}C_{TC}$ can be represented by the relative contributions of TC from marine and continental sources times their stable carbon isotopic composition (see the equation1).

$$\delta^{13}C_{TC} = f_{TC\text{-}marine} \times \delta^{13}C_{TC\text{-}marine} + f_{TC\text{-}continent} \times \delta^{13}C_{TC\text{-}continent} \quad (3)$$

$$f_{TC\text{-}marine} + f_{TC\text{-}continent} = 1 \quad (4)$$

Before assessing the relative contribution of continental versus marine TC, we need to understand the likely variability associated with the end-member stable carbon isotopic composition and the factors affecting it.

Radiocarbon based source apportionment of TC over the IGP (Kanpur: 77%; Hisar: 81%; Manora Peak: 82%), other receptor sites in South Asia (Ahmedabad: 68%; Sinhagad: 64%) and the South Asian outflow sampled over a remote island in the tropical Indian Ocean (Maldives:68%) altogether revealed that biomass burning/biogenic sources mostly dominate the source-emissions (Sheesley et al., 2012; Bosch et al., 2014; Bikkina et al., 2017a). This means that the TC isotopic composition is largely governed by the biomass component over South Asia and its outflow to the Arabian Sea. Globally, significant differences were observed between the two major plant biomasses in which the globally dominant C_3 vegetation (i.e., mostly trees) are characterized by lower $\delta^{13}C$ values (-24‰ to -30‰) than the less abundant C_4 vegetation (*e.g.,* shrubs, grasses, wheat, corn, and maize; -12 to -18‰)(Cachier et al., 1986)). Because of this persistent difference in the stable carbon isotopic composition of C_3 and C_4 land vegetation, it is important to understand their relative dominance over South Asia. Therefore, we have overlapped the C_4 vegetation (%) from Still et al. (2009) over South Asia in Figure 5a. From this figure, it is implicit that mostly C_3 plant burning is the controlling factor that dictates the $\delta^{13}C_{TC}$ values in the South Asian outflow sampled over the Arabian Sea during our winter cruise. Basu et al. (2015) have documented that C_3 plants over the IGP, India are characterized by a distinctly lower $\delta^{13}C$ values (–29.6±1.9‰) than the C_4 vegetation over this domain (–12.7±1.4‰). Besides, the $\delta^{13}C_{TC}$ in ambient aerosols collected near biomass burning emissions (i.e., mostly rice straw) in the IGP in South Asia (-26.9 to -25.4‰; median: -26.6‰; (Singh et al., 2021a)) showed consistency with those from the forest fires in Thailand, Southeast Asia (-26.0±1.2‰;(Boreddy et al., 2018)). Similarly, the wood burning emissions also contribute to similar $\delta^{13}C_{TC}$ values in the South Asian outflow (-27.6‰ to -24.9‰; (Ancelet et al., 2013); (Garbaras et al., 2015)).

As mineral dust also significantly contributes to the soil organic carbon in TSP samples collected over the Arabian Sea, we, therefore, examined the impact of mineral dust over the Arabian

Sea during the SS379 cruise based on the deduced mineral dust fraction (MDF) from the Modern-Era Retrospective analysis for Research and Applications, Version 2 (MERRA-2) simulations (Figure 5b). From the spatial variability of MDF (Figure 5b), which is a ratio of aerosol optical depth of dust to that of columnar loading of total aerosols, over the Arabian Sea it is implicit that northeasterly surface winds are rather week with some influence of mineral dust from the IGP and Thar regions. Recently, Agnihotri et al. (2020) have documented that Thar soils are enriched in carbonates and their $\delta^{13}C$ values correspond to ~-10.5±4.0‰. Therefore, it is likely that presence of dust particles in TSP over the Arabian Sea also affect the over $\delta^{13}C_{TC}$ in South Asian outflow. In contrast, the $\delta^{13}C_{TC}$ in ambient aerosols collected in road tunnels measured in China (-25.0±0.3‰; (Dai et al., 2015)), New Zealand (-25.9±0.8‰; (Ancelet et al., 2011)), and Mexico (-25.5±0.1‰; (López-Veneroni, 2009)) are much higher than that of biomass burning emissions. Likewise, the coal combustion source contributed to similar $\delta^{13}C_{TC}$ values in China, Australia, and Russia ((Felix et al., 2012; Feng et al., 2020); Table 2). Recently, Andersson et al. (2015) have constrained the likely variability in the endmember choice of $\delta^{13}C$ from biomass burning, liquid fossil (*e.g.,* gasoline, diesel) and coal combustion derived TC based on the existing literature as -26.7±1.8‰, -25.5±1.3‰, and -23.4±1.3‰. Given the predominance of biomass burning/biogenic source emission to ambient TC over South Asia and its outflow to the tropical Indian Ocean (~80%) based on radiocarbon isotope constrained source apportionment (Bikkina et al., 2017a), we assumed that the remaining 20% share of ambient TC is because of the near equal source strength of two major fossil fuel combustion sources (*e.g.,* coal and gasoline/diesel) the continental outflow from South Asia. Combining these fractions with the endmember $\delta^{13}C$ values of respective source emissions from the Andersson et al. (2015), we coherently arrived a $\delta^{13}C_{TC}$ for the continental signature (~ –26.3‰).

Cachier et al. (1986) and their predecessors (Descolas-Gros and Fontungne, 1990) observed that the $\delta^{13}C$ of carbon particles associated with seasalt particles over a marine basin is closely related to that of phytoplankton biomass in the underlying surface waters. Besides, Fontugne and Duplessy (1981) pointed out that $\delta^{13}C$ of plankton community is somewhat dependent on the temperature of the waters. As a consequence, the $\delta^{13}C$ values of planktons from the temperate and tropical oceans lie between -22‰ and -18‰, whereas those belong to high latitudes (for *e.g.,* Antarctic Ocean) and upwelling domains are characterized by lower $\delta^{13}C$ (-30‰ to -25‰) and higher $\delta^{13}C$ (-20‰ to -14‰), respectively. Recently, it has been observed that there is significant discrepancy in the $\delta^{13}C$ values of seaspray aerosols enriched with the organic matter produced under low (-20‰ to -23‰) and high biologically active oceanic waters (-20‰ to -18‰; (Crocker et al.,

2020)). Buat-Manard (1989) have elaborated the $\delta^{13}C$ variability of particulate organic carbon in marine aerosols from the peru upwelling coast and remote oceanic regions ($\delta^{13}C_{TC}$: -22 to -18‰). One interesting aspect of their study to reconsider here is that similar size distributions of particulate organic carbon (i.e., mostly WSOC, associated with seasalt aerosols) and Na^+ (i.e., a major ion of seasalt) concentration in marine aerosols along with their anomalous high abundance ratio of carbon to sodium (OC/Na: 0.135) for the upwelling prone marine basins such as Peru (Buat-Manard, 1989).

As the surface waters of the Arabian Sea in winter also characterized by high productivity because of the convective vertical mixing, one would expect similar enrichment of OC/Na over this marine region like Peru. Instead, we found much more high values of C/Na in marine aerosols collected over the coastal and offshore waters of the Arabian Sea during SS379 cruise (OC/Na: 2.9±2.4). More specifically, our OC/Na ratios over the Arabian Sea are much higher than those reported over the Peru upwelling coast. This is mainly because of the impact of South Asian outflow on the former marine basin during winter season (Kumar et al., 2008b; Bikkina et al., 2020a). Therefore, the continental OC aerosols largely dictate the $\delta^{13}C_{TC}$ over the Arabian Sea. Overall, we used $\delta^{13}C_{TC\text{-}marine}$ as −21±2‰ and $\delta^{13}C_{TC\text{-}continent}$ as -26±2‰ for estimating the relative contribution of TC from continental and marine sources over the Arabian Sea during our winter cruise.

This calculation has revealed that 69±16% of TC originates from continents. We emphasize that there is an inherent assumption related to no change in endmember isotopic composition of marine and continental TC aerosols. Although independent assessment of $\delta^{13}C_{TC}$ in remote marine aerosols from various places shows only narrow spread (-21±2‰), ambient TC (*i.e.*, mass analog of OAs) evolve continuously via the oxidation and/or secondary formation processes. Of these contrasting processes, that is degradation of OC causing loss of small carbon moieties to gas phase and secondary formation adds up to the OC mass, oxidation of TC dominates the latter phenomenon. If the $\delta^{13}C_{TC\text{-}continent}$ is affected by the source-emissions and subsequently modified by oxidation during transport, we would underestimate the fraction of TC from the continental outflow. This means that continental (anthropogenic/biogenic) sources contribute more than 70% of TC over the Arabian Sea.

There also exists a remarkable inverse temporal trend between $\delta^{13}C_{TC}$ and WIOC concentrations over the Arabian Sea. TC in atmospheric aerosols is comprises of both water-soluble organic carbon (WSOC), water-insoluble organic carbon (WIOC: OC-WSOC) and EC. The fraction of WSOC, in general, increases during transport because of the oxidative degradation of TC, in which WIOC becomes more WSOC. Nevertheless, this process causes enrichment of $^{13}C_{TC}$, resulting

in a somewhat higher $\delta^{13}C_{TC}$ during transport than those observed over the source-emissions. In such a scenario, we could expect that oxidation of OAs during transport simultaneously modify WIOC pool, affecting the overall $\delta^{13}C_{TC}$. Coincidently, we observed lower WIOC to be associated with higher $\delta^{13}C_{TC}$ (~–23‰) and vice versa (*i.e.*, higher WIOC is associated with lower $\delta^{13}C_{TC}$ from the source-emissions, per se centering on–26‰).

3.6. Source apportionment

We have compared the $\delta^{13}C_{TC}$ and $\delta^{15}N_{TN}$ in the air over the Arabian Sea with those relevant for the source emissions to underpin the possible sources of organic aerosols (Turekian et al., 1998; Agnihotri et al., 2011a; Górka et al., 2014; Garbaras et al., 2015; Morera-Gómez et al., 2018) and their mixing with the inorganic aerosol components during continental outflow (Figure 6a). The $\delta^{13}C$-$\delta^{15}N$ isospace plot in Figure 6a has revealed that major contributing sources of TC and TN over the Arabian Sea are biomass burning (i.e., mostly C_3 vegetation) and coal fired power plants in South Asia. Furthermore, we employed a Bayesian approach based stable isotope-mixing model ((Simmr, 2020), (Parnell A., 2020)) to assess the proportional contribution of TC and TN from various source-emissions (C_3/C_4 biomass, phytoplankton, coal, and vehicles) in marine aerosols collected over the Arabian Sea during the winter cruise (SS-379). For this study, we used the endmember $\delta^{13}C$ and $\delta^{15}N$ values of various source-emissions from the literature as an input to the Simmr model. These sources include particles originated from the phytoplankton ($\delta^{13}C_{phyto}$:-21.0±1.9‰(Miyazaki et al., 2011); $\delta^{15}N_{phyto}$: 4.9±2.8‰(Miyazaki et al., 2011)), coal combustion ($\delta^{13}C_{coal}$: -23.4±1.3‰(Heaton, 1990; Feng et al., 2020); $\delta^{15}N_{coal}$: 8.7±0.5‰(Felix et al., 2012; Feng et al., 2020)), vehicular emissions ($\delta^{13}C_{vehicle}$: -25.5±1.3‰ ((Heaton, 1990; Dai et al., 2015); $\delta^{15}N_{vehicle}$: 5.7±2.8‰ ((Heaton, 1990)), C_3 plants ($\delta^{13}C_{C3biomass}$: -26.7±1.8‰ ((Andersson et al., 2015); $\delta^{15}N_{C3biomass}$: +19.4±2.1‰((Boreddy et al., 2018)), and soil dust ($\delta^{13}C$: -10.5±4.0‰, $\delta^{15}N$: +11.3±1.6‰; (Agnihotri et al., 2020)). Our choice of endmembers are very much comparable with literature reports for source emissions in terms of their $\delta^{13}C$ (Table 3) and $\delta^{15}N$ (Table 4). In the Simmr model, the data for $\delta^{13}C_{TC}$ and $\delta^{15}N_{TN}$ of the TSP from the Arabian Sea has been taken as an input and the model iteratively solves the mixing equations related to source contributions from the specified endmember $\delta^{13}C$ and $\delta^{15}N$ values alongside taking into the effect of fractionation using the markov-chian Monte carlo methods. Here, the $\delta^{13}C$-$\delta^{15}N$ isospace plot clearly revealed the predominance of TC from the C_3 biomass burning emissions. Besides, the Simmr algorithm clearly deconvoluted the dominance of TC and TN from the C_3 biomass burning (69±5%), vehicle exhaust (8±5%), coal fired power plants (10±6%). All other continental *(e.g.*, dust: 5±2%) and marine sources *(i.e.*,

phytoplankton exudates or related organic matter from seas: 8±5%) are only minor components (Figure 6b).

3.7. Processes affecting $\delta^{13}C_{TC}$

In the atmosphere, organic aerosols undergo oxidation (*aka* aging) during long-range transport and become more water-soluble. This is because of the prolonged oxidation of airborne particulate organic matter in which the constituent carbon atoms are attacked by more oxidants (*e.g.*, OH groups), converted to WSOC (Aggarwal and Kawamura, 2008; Kirillova et al., 2013; Pavuluri and Kawamura, 2016; Bikkina et al., 2017a; Bikkina et al., 2019b). Another process that could influence the abundances of WSOC during atmospheric transport is the formation of secondary organic aerosols (SOA). Generally, wintertime meteorological conditions (shallow atmospheric boundary layer, more polluted precursor compounds and aqueous-phase medium) make favor for the formation of secondary organic aerosols. Therefore, it is very likely that variations in $\delta^{13}C$ are linked to changes in secondary aerosol formation rate too, in addition to aging process (Fu et al., 2012; Rastogi et al., 2020). Many studies have observed a significant positive linear relationship between SOA tracers (*e.g.*, oxalic acid) and WSOC and, hence, argued that organic aerosols formed by the condensation of semivolatile organic precursors become more water-soluble in nature (Bikkina et al., 2017b). As a result, the WSOC/TC ratio observed in source-emission increases during long-range transport (Ram et al., 2010). However, aging of organic aerosols (*i.e.*, formed either by the oxidation or secondary process) significantly affects their stable carbon isotopic composition (*i.e.*, can be represented by the $\delta^{13}C_{TC}$). If the aging process influences the atmospheric abundances of organic aerosols collected over the Arabian Sea during our winter cruise, then we would expect some sort of relationship between WSOC/TC ratios and $\delta^{13}C_{TC}$. Depending on the prevalent positive or negative linear relationship, we can ascertain the relative significance of the secondary formation process in the atmosphere during the continental outflow to the Arabian Sea (Bikkina et al., 2019b).

In general, the oxidation process involves a loss of lighter carbon-containing isotopologues of small carbon moieties (*e.g.*, $^{12}CO_2$) to gas phase and causes a ^{13}C enrichment in the remaining organic aerosols (Kirillova et al., 2013). This means that oxidation process of organic aerosols often results in higher $\delta^{13}C_{TC}$. On the other hand, volatile organic compounds (VOCs) emitted from biogenic and anthropogenic sources are oxidized in the atmosphere by the ambient oxidants (*e.g.*, O_3, $^{\bullet}OH$ and $NO_2^{\bullet}$ radicals) to form semi/low volatile organic compounds (SVOCs) (Irei et al., 2006; Irei et al., 2011). During this process, the ^{12}C-containing VOCs preferentially react with the oxidants to form SVOCs because of the KIE (Irei et al., 2006; Irei et al., 2011), which eventually condenses to yield

SOA (Iannone et al., 2003; Anderson et al., 2004a; Anderson et al., 2004b). Consequently, SOA component is characterized by lower $\delta^{13}C$ values (Kirillova et al., 2013; Bikkina et al., 2019b) than anthropogenic/biogenic precursor VOCs (Anderson et al., 2004a; Anderson et al., 2004b; Irei et al., 2006; Kirillova et al., 2013; Bikkina et al., 2019b). If we presume that both oxidation and secondary formation processes occurring simultaneously over the Arabian Sea, then their relative importance dictates the $\delta^{13}C_{TC}$ in marine aerosols.

We have observed a positive linear relationship between WSOC/TC and $\delta^{13}C_{TC}$ over the Arabian Sea (Figure 7a). Irrespective of TC content, the proportions of WSOC in TC here exhibited a positive linear relationship with the $\delta^{13}C_{TC}$. Similar relationship between WSOC/TC and $\delta^{13}C_{TC}$ has been observed for the wintertime aerosols in Mumbai, a coastal megacity along the western India during the impact of polluted air masses from the IGP (Aggarwal et al., 2013b). As the aging process or oxidation of organic aerosols during transport make them more water-soluble, then there is an increase in WSOC mass. This means that TC contains less WSOC in the source emission than it does during transport (*i.e.,* having higher WSOC/TC ratios). We assume that organic aerosols from the wintertime haze pollution in South Asia are advected to the Arabian Sea by the prevailing northwesterly winds to initiate the aging process. The oxidation processes result in an enrichment of ^{13}C in gas phase, leading to higher $\delta^{13}C$ of OA than the precursor organics (Bikkina et al., 2019b). In contrast, SOAs formed by the condensation of SVOCs (*i.e.,* depleted in ^{13}C because of the KIE) on to a preexisting airborne particulate matter can contribute to lower $\delta^{13}C$ (Irei et al., 2006; Kirillova et al., 2013; Bikkina et al., 2019b). By considering these processes associated with the oxidation of OA, we argue that the prevalent positive linear relationship between WSOC/TC and $\delta^{13}C_{TC}$ over the Arabian Sea is mainly caused by atmospheric oxidation of organic aerosols during long-range transport from South Asia.

3.8. Processes affecting $\delta^{15}N_{TN}$

The $\delta^{15}N_{TN}$ in marine aerosols over the Arabian Sea during the winter cruise is somewhat governed by the constituent nitrogenous components. Because of the predominance of NH_4^+ over NO_3^- and organic nitrogen (ON) in TN, atmospheric processes affecting its abundance govern the $\delta^{15}N_{TN}$. The chemical reactions of NH_3 with acidic species (*e.g.,* H_2SO_4 and HNO_3) formed by the oxidation of SO_2 and NO_x gases produce ammonium sulfate/bisulfate and/or ammonium nitrate aerosols.

$$2NH_3\,(g) + H_2SO_4(l) \rightarrow (NH_4)_2SO_4(p) \qquad (5)$$

$$NH_3(g) + H_2SO_4(l) \rightarrow NH_4HSO_4(p) \quad (6)$$

$$NH_3(g) + HNO_3(l) \rightleftharpoons NH_4NO_3(p) \quad (7)$$

$$CaCO_3\,(p) + 2HNO_3\,(l) \rightarrow Ca(NO_3)_2(p) + CO_2 + H_2O \quad (8)$$

The chemical form in which NH_3 exists in the atmosphere can be traced by the relationship of NH_4^+ with non-sea-salt or nss-SO_4^{2-} and NO_3^- in aerosols. Based on the linear regression analysis between NH_4^+ and nss-SO_4^{2-} in the TSP samples from SS379 cruise, we ascertained the prevalence of NH_4HSO_4 or $(NH_4)_2SO_4$ in aerosols (Bikkina et al., 2020a). We found that the average equivalent mass ratio of NH_4^+/nss-SO_4^{2-} over the Arabian Sea during the cruise is far less than unity (0.55±0.25), indicating ammonia-deficit conditions. This observation implies that marine aerosols over the Arabian Sea likely contain both the forms, NH_4HSO_4 or $(NH_4)_2SO_4$. In this study, we found a negative linear relationship between $\delta^{15}N_{TN}$ and the equivalent mass ratios of NH_4^+ to nss-SO_4^{2-} over the Arabian Sea (Figure 7b). Similar relationships were observed over the Bay of Bengal and other geographical locations in India (Mumbai: +22.8±1.4‰; (Aggarwal et al., 2013a); Chennai: day: +25.5±2.4‰; night: +23.0±2.3‰; (Pavuluri et al., 2010)) and Europe (Vodička et al., 2019). Notably, the aerosols sampled in all these studies are influenced by the BB emissions in the South Asian outflow. A remarkable distinction was observed in terms of higher $\delta^{15}N_{TN}$ values in the South Asian outflow to the Arabian Sea (av. 19.5±2.1‰) and the Bay of Bengal (+20.4±5.4‰) in winter season as compared to the East Asian outflow to the East China Sea (+0.7±3.3‰; (Xiao et al., 2018)), Okinawa island, Japan (13.6±1.72‰;(Kunwar et al., 2016)) and to the Western North Pacific (Seoul, S. Korea: 13.3±2.7‰; (Park et al., 2018); Jeju island, S. Korea: +15.1±3.4‰; (Kundu et al., 2010b)). This is probably caused by the predominance of NH_4^+ over other nitrogen components (NO_3^- and N_{Org}) in the wider South Asian outflow and the extent of its reaction with major acidic species (H_2SO_4) of ambient aerosols. Heaton (1990) observed that aerosol filters when loaded with liquid NH_3 are exposed to sulfuric acid (H_2SO_4) fumes have caused significant enrichment of $\delta^{15}N_{TN}$ (up to +33‰) in the resulted ammonium sulphate aerosols. This means the extent of reaction of NH_3 with H_2SO_4 (Eqn 3) in the continental outflows to the Arabian Sea governs the overall $\delta^{15}N_{TN}$. Furthermore, the aging effect on aerosols is more pronounced in the South Asian outflow mainly because of the downwind transport (20°N to 0°N/E) compared to the lateral advection of air pollutants from East Asia to the Western North Pacific. As such, the differences in atmospheric abundances of aerosol-N as well as the $\delta^{15}N_{TN}$ of marine aerosols from the South and East Asian outflow are, in part, could be attributed to variable weather conditions between South Asia and East Asia (e.g., Temp & RH).

Ammonium nitrate (NH_4NO_3) in ambient aerosols is always in equilibrium with its precursors (NH_3 and HNO_3) (Jickells, 2006). However, NH_4NO_3 reverts to its precursors during transport due to a rapid loss of NH_3 to the surface. This is mainly because of the highly volatile nature of NH_4NO_3 and high deposition velocity of gasesous NH_3 in the ambient atmosphere (Jickells, 2006). As a result, no such significant linear relationship was observed between NH_4^+ and NO_3^- over the Arabian Sea. In contrast, NO_3^- is usually associated with coarse mode mineral dust and/or sea salt particles in the atmosphere (Mamane and Gottlieb, 1992; Wu and Okada, 1994; Jickells, 2006). We have observed a moderate significant linear relationship between NO_3^- and nss-Ca^{2+}, which is a potential proxy of mineral dust (Rastogi and Sarin, 2006; Chen et al., 2007; Kumar et al., 2008a; Bikkina and Sarin, 2012) in our TSP samples collected over the Arabian Sea. This observation suggests the reactive uptake of HNO_3 on mineral dust particles during the continental outflow to the Arabian Sea (Eqn 5). Similar to $\delta^{13}C_{TC}$, we also measured the $\delta^{15}N_{TN}$ of the acid-exposed filters for the concentration and isotopic composition of remaining nitrogen ($TN_{remained}$ and $\delta^{15}N_{TN\text{-}remained}$, respectively). By comparing the $TN_{remained}$ with TN and using the isotope mass balance equation, we have estimated the removed nitrogen component ($TN_{removed}$) and the associated stable nitrogen isotopic composition ($\delta^{15}N_{TN\text{-}removed}$).

$$TN_{removed} = TN - TN_{remained} \quad (9)$$

$$\delta^{15}N_{TNremoved} = (TN \times \delta^{15}_{TN} - TN_{remained} \times \delta^{15}N_{TN\text{-}remained})/TN_{removed} \quad (10)$$

We observed a strong positive linear relationship of $TN_{remained}$ with NH_4^+-N over the Arabian Sea (Figure 8a). Kawamura et al. (2004) argued that the aerosol filters when exposed to HCl fumes would expel NO_3^- without altering the abundance of NH_4^+ present in the atmospheric particulate matter. Their inference was primarily based on the strong positive linear relationships ($R^2 = 0.86$) observed between NH_4^+-N and $TN_{remained}$ (Kawamura et al., 2004). It is important to note the prevailing differences in the dominant chemical components of aerosol-N from this study and the Asian dust outbreaks sampled over Gosan in Jeju Island of South Korea, where TN largely consists of NH_4^+ and NO_3^-. In contrast, our observations are from the Arabian Sea during a winter cruise where the pollution-derived NH_4^+, NO_3^- and ON contribute disproportionately to TN in marine aerosols. Indeed, ON is the second most abundant nitrogenous component after NH_4^+ in the TSP samples collected over the Arabian Sea during the present cruise. Therefore, the linear regression slope of $TN_{remained}$ with NH_4^+ was 0.90 (Figure 8a). We also observed a significant positive correlation between $TN_{removed}$ and nss-sea-salt Ca^{2+} (Figure 8b) as well as that was found between

NO_3^- and nss-Ca^{2+} (Bikkina et al., 2021), suggesting that the expelled component is likely the NO_3^- component of aerosols.

Another important feature worth discussing here that the low TC/TN ratios and corresponding high $\delta^{15}N_{TN}$ over the Arabian Sea in winter season (this study) were in sharp contrast to that of high TC/TN ratios and associated with rather low $\delta^{15}N_{TN}$ values observed in spring intermonsoon cruise (Agnihotri et al., 2011b). Earlier investigations have revealed a pronounced impact of continental outflow from South Asia, mainly from biomass burning and fossil-fuel combustion, on the chemical composition of marine aerosols over the Indian Ocean in winter season (Kumar et al., 2008a; Kumar et al., 2008b; Bikkina and Sarin, 2012; Aswini et al., 2020). On the other hand, spring-intermonsoon is a transition period with relatively weak influence of pollution sources in the continental outflow but with an increased contribution of mineral dust from the deserts in the Middle East and South Asia (Pease et al., 1998; Tindale and Pease, 1999; Prospero et al., 2002; Badarinath et al., 2010). Besides, the Arabian Sea is also a major hotspot region of water-column denitrification process, a microbial respiration involving the degradation of sinking phytoplankton-derived particulate organic matter by means of reducing NO_3^- to N_2O or N_2 under oxygen deficit conditions (Naqvi, 1987; Naqvi, 1991; Ward et al., 2009). These studies provide important insights regarding a major nitrogen loss across the air-sea-interface. Furthermore, Jickells et al. (2003) observed that NH_4^+ associated with sea-spray are more depleted and, hence, their contribution to marine aerosols could lead to a rather low $\delta^{15}N_{TN}$ in spring-intermonsoon season (Agnihotri et al., 2011b). In contrast, the prolonged aging of NH4+ and organic nitrogen aerosols from the BB and animal live-stock husbandry emissions are largely responsible for higher $\delta^{15}N_{TN}$. Furthermore, we also compared the available data of equivalent mass ratio of NH_4^+/SO_4^{2-} and $\delta^{15}N_{TN}$ over South Asia with those documented over East Asia (Figure S1). This comparison revealed that lower ratios of NH_4^+/SO_4^{2-} (less than unity) over South Asia were accompanied with an apparent increase in $\delta^{15}N_{TN}$ values through the heterogeneous reactions of gaseous NH_3 with sulfuric acid droplets and, hence, contributes to high $\delta^{15}N_{TN}$ values. Besides, relatively low contribution of particulate NH_4^+ and/or organic nitrogen over NO_3^- in East Asia could explain relatively low $\delta^{15}N_{TN}$ values over this geographical domain.

4. Conclusions

In this study, we present the first and foremost field based measurments on the stable carbon and nitrogen isotopic composition of bulk carbon and nitrogen in wintertime ambient marine aerosols collected over the Arabian Sea during the impact of South Asian outflow. Our results

combining with the backward air mass trajectories and MODIS fire count data have elucidated the predominance of crop-residue burning emissions in the NW. IGP and southern India. The $\delta^{13}C_{TC}$ over the Arabian Sea showed significant linear relationship with WSOC/TC, emphasizing the impact of aging (oxidation) of anthropogenic organic aerosols during long-range transport. The elevated abundance of ^{15}N and, hence, the associated high $\delta^{15}N_{TN}$ over the Arabian Sea clearly suggest the impact of biomass/biofuel burning emissions over South Asia as a result of seasonally developing "Atmospheric Brown Haze" and its influence on the tropical Indian Ocean due to the meteorology. Besides, we also noticed a significant inverse linear relationship between $\delta^{15}N_{TN}$ and equaivalent mass ratios of NH_4^+ to ($nss\text{-}SO_4^{2-}$), suggesting that heterogeneous particle formation of gaseous NH_3 with sulfuric acid droplets. Furthermore, we employed stable isotope mixing model in R under the Bayesian frame work to the $\delta^{13}C$ and $\delta^{15}N$ data to ascertain the relative contribution of organic aerosols from various sources including those continental and marine ones. This analysis revealed that C_3 biomass burning is the major contributor (~69±5%) followed by coal fired power plants (10±6%), vehicular exhaust (8±5%), phytoplankton derived marine organic matter (8±5%), and mineral dust (5±2%). All these results based on the $\delta^{13}C_{TC}$ and $\delta^{15}N_{TN}$ over the Arabain Sea have strongly advocated the impact of processes affecting the atmospheric abundances of organic aerosols in the South Asian outflow.

Acknowledgements

PB acknowledges the partial financial support from the DST-INSPIRE fellowship (DST/INSPIRE/04/2017/000324 dated 24/07/2017) and JASSO (Japan Student Service Organization) Followup research fellowship 2019. PB is grateful to the Director of NIO for the support at the workplace. PB is also thankful to the Ship Captain and crew for their support during the cruise. Authors are thankful to the Chief Scientist Dr. GVM Gupta (CMLRE, Kochi) and participants onboard of SS379 for their help in the sampling. Authors thankfully acknowledge the NOAA Air Resources Laboratory for the access to the HYSPLIT model (http://www.arl.noaa.gov/ready.html). We also acknowledge NASA's Goddard Earth Sciences Data and Information Services Center for providing access to MODIS aerosol optical depth and fire count data from the GES-DISC Interactive Online Visualization and analysis portal.

References

Achyuthan H, Quade J, Roe L, Placzek C. Stable isotopic composition of pedogenic carbonates from the eastern margin of the Thar Desert, Rajasthan, India. Quaternary International 2007; 162-163: 50-60.

Aggarwal S, Kawamura K, Umarji G, Tachibana E, Patil R, Gupta P. Organic and inorganic markers and stable C-, N-isotopic compositions of tropical coastal aerosols from megacity Mumbai: sources of organic aerosols and atmospheric processing. Atmospheric Chemistry and Physics 2013a; 13: 4667-4680.

Aggarwal SG, Kawamura K. Molecular distributions and stable carbon isotopic compositions of dicarboxylic acids and related compounds in aerosols from Sapporo, Japan: Implications for photochemical aging during long-range atmospheric transport. Journal of Geophysical Research: Atmospheres 2008; 113: doi: 10.1029/2007JD009365.

Aggarwal SG, Kawamura K, Umarji GS, Tachibana E, Patil RS, Gupta PK. Organic and inorganic markers and stable C-, N-isotopic compositions of tropical coastal aerosols from megacity Mumbai: sources of organic aerosols and atmospheric processing. Atmos. Chem. Phys. 2013b; 13: 4667-4680.

Agnihotri R, Karapurkar SG, Sarma VV, Yadav K, Kumar MD, Sharma C, et al. Stable Isotopic and Chemical Characteristics of Bulk Aerosols during Winter and Summer Season at a Station in Western Coast of India (Goa). Aerosol and Air Quality Research 2015; 15: 888-900.

Agnihotri R, Mandal T, Karapurkar S, Naja M, Gadi R, Ahammmed YN, et al. Stable carbon and nitrogen isotopic composition of bulk aerosols over India and northern Indian Ocean. Atmospheric Environment 2011a; 45: 2828-2835.

Agnihotri R, Mandal TK, Karapurkar SG, Naja M, Gadi R, Ahammmed YN, et al. Stable carbon and nitrogen isotopic composition of bulk aerosols over India and northern Indian Ocean. Atmospheric Environment 2011b; 45: 2828-2835.

Agnihotri R, Sawlani R, Azam M, Basumatary S, Sharma C, Mishra S, et al. Geochemical, stable isotopic, palynological characterization of surface dry soils and atmospheric particles over Jodhpur city (Thar Desert, Rajasthan) during peak summer of 2013. MAPAN 2020; 35: 53-67.

Aguilera J, Whigham LD. Using the 13C/12C carbon isotope ratio to characterise the emission sources of airborne particulate matter: a review of literature. Isotopes in Environmental and Health Studies 2018; 54: 573-587.

Ancelet T, Davy PK, Trompetter WJ, Markwitz A, Weatherburn DC. Carbonaceous aerosols in an urban tunnel. Atmospheric Environment 2011; 45: 4463-4469.

Ancelet T, Davy PK, Trompetter WJ, Markwitz A, Weatherburn DC. Carbonaceous aerosols in a wood burning community in rural New Zealand. Atmospheric Pollution Research 2013; 4: 245-249.

Anderson RS, Huang L, Iannone R, Thompson AE, Rudolph J. Carbon Kinetic Isotope Effects in the Gas Phase Reactions of Light Alkanes and Ethene with the OH Radical at 296 ± 4 K. The Journal of Physical Chemistry A 2004a; 108: 11537-11544.

Anderson RS, Iannone R, Thompson AE, Rudolph J, Huang L. Carbon kinetic isotope effects in the gas-phase reactions of aromatic hydrocarbons with the OH radical at 296 ± 4 K. Geophysical Research Letters 2004b; 31: 10.1029/2004GL020089.

Andersson A, Deng J, Du K, Zheng M, Yan C, Sköld M, et al. Regionally-varying combustion sources of the January 2013 severe haze events over eastern China. Environmental science & technology 2015; 49: 2038-2043.

Aswini AR, Hegde P, Aryasree S, Girach IA, Nair PR. Continental outflow of anthropogenic aerosols over Arabian Sea and Indian Ocean during wintertime: ICARB-2018 campaign. Science of The Total Environment 2020; 712: 135214.

Badarinath KVS, Kharol SK, Kaskaoutis DG, Sharma AR, Ramaswamy V, Kambezidis HD. Long-range transport of dust aerosols over the Arabian Sea and Indian region — A case study using satellite data and ground-based measurements. Global and Planetary Change 2010; 72: 164-181.

Basu S, Agrawal S, Sanyal P, Mahato P, Kumar S, Sarkar A. Carbon isotopic ratios of modern C3–C4 plants from the Gangetic Plain, India and its implications to paleovegetational reconstruction. Palaeogeography, Palaeoclimatology, Palaeoecology 2015; 440: 22-32.

Bikkina P, Kawamura K, Bikkina S, Kunwar B, Tanaka K, Suzuki K. Hydroxy Fatty Acids in Remote Marine Aerosols over the Pacific Ocean: Impact of Biological Activity and Wind Speed. ACS Earth and Space Chemistry 2019a; 3: 366-379.

Bikkina P, Sarma VVSS, Kawamura K, Bikkina S. Dry-deposition of inorganic and organic nitrogen aerosols to the Arabian Sea: Sources, transport and biogeochemical significance in surface waters. Marine Chemistry 2021; 231: 103938.

Bikkina P, Sarma VVSS, Kawamura K, Bikkina S, Kunwar B, Sherin CK. Chemical characterization of wintertime marine aerosols over the Arabian Sea: Impact of marine sources and long-range transport. Atmospheric Environment 2020a: 117749.

Bikkina S, Andersson A, Ram K, Sarin MM, Sheesley RJ, Kirillova EN, et al. Carbon isotope-constrained seasonality of carbonaceous aerosol sources from an urban location (Kanpur) in the Indo-Gangetic Plain. Journal of Geophysical Research: Atmospheres 2017a; 122: 4903-4923.

Bikkina S, Andersson A, Sarin MM, Sheesley RJ, Kirillova E, Rengarajan R, et al. Dual carbon isotope characterization of total organic carbon in wintertime carbonaceous aerosols from northern India. Journal of Geophysical Research: Atmospheres 2016a; 121: 4797-4809.

Bikkina S, Haque MM, Sarin M, Kawamura K. Tracing the relative significance of primary versus secondary organic aerosols from biomass burning plumes over Coastal Ocean using sugar compounds and stable carbon isotopes. ACS Earth and Space Chemistry 2019b.

Bikkina S, Kawamura K, Sarin M. Stable carbon and nitrogen isotopic composition of fine mode aerosols (PM 2.5) over the Bay of Bengal: impact of continental sources. Tellus B 2016b; 68: doi:10.3402/tellusb.v68.31518.

Bikkina S, Kawamura K, Sarin M. Secondary organic aerosol formation over Coastal Ocean: Inferences from atmospheric water-soluble low molecular weight organic compounds. Environmental Science & Technology 2017b; 51: 4347–4357.

Bikkina S, Kawamura K, Sarin M, Tachibana E. 13C Probing of Ambient Photo-Fenton Reactions Involving Iron and Oxalic Acid: Implications for Oceanic Biogeochemistry. ACS Earth and Space Chemistry 2020b.

Bikkina S, Sarin M. Atmospheric pathways of phosphorous to the Bay of Bengal: contribution from anthropogenic sources and mineral dust. Tellus B 2012; 64.

Bikkina S, Sarin M, Kumar A. Impact of anthropogenic sources on aerosol iron solubility over the Bay of Bengal and the Arabian Sea. Biogeochemistry 2012; 110: 257-268.

Bikkina S, Sarin MM, Rengarajan R. Atmospheric transport of mineral dust from the Indo-Gangetic Plain: Temporal variability, acid processing, and iron solubility. Geochemistry, Geophysics, Geosystems 2014; 15: 3226-3243.

Bikkina S, Sarin MM, Sarma VVSS. Atmospheric dry deposition of inorganic and organic nitrogen to the Bay of Bengal: Impact of continental outflow. Marine Chemistry 2011; 127: 170-179.

Boreddy SKR, Parvin F, Kawamura K, Zhu C, Lee C-T. Stable carbon and nitrogen isotopic compositions of fine aerosols (PM2.5) during an intensive biomass burning over Southeast Asia: Influence of SOA and aging. Atmospheric Environment 2018; 191: 478-489.

Bosch C, Andersson A, Kirillova EN, Budhavant K, Tiwari S, Praveen P, et al. Source-diagnostic dual-isotope composition and optical properties of water-soluble organic carbon and elemental carbon in the South Asian outflow intercepted over the Indian Ocean. Journal of Geophysical Research: Atmospheres 2014; 119: 11,743-11,759.

Buat-Manard P. Sources of particulate carbon in the marine atmosphere. Chemical oceanography 1989; 10: 251-279.

Cachier H, Buat-Ménard P, Fontugne M, Chesselet R. Long-range transport of continentally-derived particulate carbon in the marine atmosphere: Evidence from stable carbon isotope studies. Tellus B 1986; 38: 161-177.

Cao J-j, Chow JC, Tao J, Lee S-c, Watson JG, Ho K-f, et al. Stable carbon isotopes in aerosols from Chinese cities: Influence of fossil fuels. Atmospheric Environment 2011; 45: 1359-1363.

Cao JJ, Zhu CS, Chow JC, Liu WG, Han YM, Watson JG. Stable carbon and oxygen isotopic composition of carbonate in fugitive dust in the Chinese Loess Plateau. Atmospheric Environment 2008; 42: 9118-9122.

Chen B, Jie D, Shi M, Gao P, Shen Z, Uchida M, et al. Characteristics of 14C and 13C of carbonate aerosols in dust storm events in China. Atmospheric Research 2015; 164-165: 297-303.

Chen W-N, Chang S-Y, Chou CCK, Chen Y-W, Chen J-P. Study of relationship between water-soluble Ca2+ and lidar depolarization ratio for spring aerosol in the boundary layer. Atmospheric Environment 2007; 41: 1440-1455.

Chesselet R, Fontugne M, Buat-Ménard P, Ezat U, Lambert CE. The origin of particulate organic carbon in the marine atmosphere as indicated by its stable carbon isotopic composition. Geophysical Research Letters 1981; 8: 345-348.

Crocker DR, Hernandez RE, Huang HD, Pendergraft MA, Cao R, Dai J, et al. Biological Influence on δ13C and Organic Composition of Nascent Sea Spray Aerosol. ACS Earth and Space Chemistry 2020; 4: 1686-1699.

Dai S, Bi X, Chan LY, He J, Wang B, Wang X, et al. Chemical and stable carbon isotopic composition of PM_{2.5} from on-road vehicle emissions in the PRD region and implications for vehicle emission control policy. Atmos. Chem. Phys. 2015; 15: 3097-3108.

Descolas-Gros C, Fontungne M. Stable carbon isotope fractionation by marine phytoplankton during photosynthesis. Plant, Cell & Environment 1990; 13: 207-218.

Draxler RR. Forecasting dust storms using Hysplit. Proceedings of Sino-US Workshop on Dust Storms and Their Effects on Human Health, November, 2002, pp. 25-26.

Elliott EM, Yu Z, Cole AS, Coughlin JG. Isotopic advances in understanding reactive nitrogen deposition and atmospheric processing. Science of The Total Environment 2019; 662: 393-403.

Fang W, Du K, Andersson A, Xing Z, Cho C, Kim S-W, et al. Dual-Isotope Constraints on Seasonally Resolved Source Fingerprinting of Black Carbon Aerosols in Sites of the Four Emission Hot Spot Regions of China. Journal of Geophysical Research: Atmospheres 2018; 0.

Felix JD, Elliott EM, Shaw SL. Nitrogen Isotopic Composition of Coal-Fired Power Plant NOx: Influence of Emission Controls and Implications for Global Emission Inventories. Environmental Science & Technology 2012; 46: 3528-3535.

Feng L, Li H, Yan D. A Refinement of Nitrogen Isotope Analysis of Coal Using Elemental Analyzer/Isotope Ratio Mass Spectrometry and the Carbon and Nitrogen Isotope Compositions of Coals Imported in China. ACS Omega 2020; 5: 7636-7640.

Fontugne M, Duplessy J. Organic-carbon isotopic fractionation by marine plankton in the temperature-range-1 to 31-degrees c. Oceanologica Acta 1981; 4: 85-90.

Fu P, Kawamura K, Chen J, Li J, Sun Y, Liu Y, et al. Diurnal variations of organic molecular tracers and stable carbon isotopic composition in atmospheric aerosols over Mt. Tai in the North China Plain: an influence of biomass burning. Atmospheric Chemistry and Physics 2012; 12: 8359-8375.

Fuzzi S, Andreae M, Huebert B, Kulmala M, Bond T, Boy M, et al. Critical assessment of the current state of scientific knowledge, terminology, and research needs concerning the role of organic aerosols in the atmosphere, climate, and global change. Atmospheric Chemistry and Physics 2006; 6: 2017-2038.

Garbaras A, Masalaite A, Garbariene I, Ceburnis D, Krugly E, Remeikis V, et al. Stable carbon fractionation in size-segregated aerosol particles produced by controlled biomass burning. Journal of Aerosol Science 2015; 79: 86-96.

Górka M, Rybicki M, Simoneit BRT, Marynowski L. Determination of multiple organic matter sources in aerosol PM10 from Wrocław, Poland using molecular and stable carbon isotope compositions. Atmospheric Environment 2014; 89: 739-748.

Guazzotti SA, Suess DT, Coffee KR, Quinn PK, Bates TS, Wisthaler A, et al. Characterization of carbonaceous aerosols outflow from India and Arabia: Biomass/biofuel burning and fossil fuel combustion. Journal of Geophysical Research: Atmospheres 2003; 108: doi: 10.1029/2002JD003277.

Gustafsson Ö, Kruså M, Zencak Z, Sheesley RJ, Granat L, Engström E, et al. Brown clouds over South Asia: biomass or fossil fuel combustion? Science 2009; 323: 495-498.

Heaton tHE. 15N/14N ratios of NOx from vehicle engines and coal-fired power stations. Tellus B 1990; 42: 304-307.

Huebert BJ, Charlson RJ. Uncertainties in data on organic aerosols. Tellus B: Chemical and Physical Meteorology 2000; 52: 1249-1255.

Iannone R, Anderson RS, Rudolph J, Huang L, Ernst D. The carbon kinetic isotope effects of ozone-alkene reactions in the gas-phase and the impact of ozone reactions on the stable carbon isotope ratios of alkenes in the atmosphere. Geophysical Research Letters 2003; 30: doi: 10.1029/2003GL017221.

Irei S, Huang L, Collin F, Zhang W, Hastie D, Rudolph J. Flow reactor studies of the stable carbon isotope composition of secondary particulate organic matter generated by OH-radical-induced reactions of toluene. Atmospheric Environment 2006; 40: 5858-5867.

Irei S, Rudolph J, Huang L, Auld J, Hastie D. Stable carbon isotope ratio of secondary particulate organic matter formed by photooxidation of toluene in indoor smog chamber. Atmospheric Environment 2011; 45: 856-862.

Jacobson MC, Hansson HC, Noone KJ, Charlson RJ. Organic atmospheric aerosols: Review and state of the science. Reviews of Geophysics 2000; 38: 267-294.

Jickells T. The role of air-sea exchange in the marine nitrogen cycle. Biogeosciences 2006; 3: 271-280.

Jickells TD, Kelly SD, Baker AR, Biswas K, Dennis PF, Spokes LJ, et al. Isotopic evidence for a marine ammonia source. Geophysical Research Letters 2003; 30.

Jimenez JL, Canagaratna MR, Donahue NM, Prévôt ASH, Zhang Q, Kroll JH, et al. Evolution of Organic Aerosols in the Atmosphere. Science 2009; 326: 1525-1529.

Kanakidou M, Seinfeld JH, Pandis SN, Barnes I, Dentener FJ, Facchini MC, et al. Organic aerosol and global climate modelling: a review. Atmos. Chem. Phys. 2005; 5: 1053-1123.

Kawamura K, Kobayashi M, Tsubonuma N, Mochida M, Watanabe T, Lee M. Organic and inorganic compositions of marine aerosols from East Asia: Seasonal variations of water-soluble dicarboxylic acids, major ions, total carbon and nitrogen, and stable C and N isotopic composition. Vol 9: The Geochemical Society, 2004.

Kirillova EN, Andersson A, Han J, Lee M, Gustafsson Ö. Sources and light absorption of water-soluble organic carbon aerosols in the outflow from northern China. Atmospheric Chemistry and Physics 2014a; 14: 1413-1422.

Kirillova EN, Andersson A, Sheesley RJ, Kruså M, Praveen P, Budhavant K, et al. 13C-and 14C-based study of sources and atmospheric processing of water-soluble organic carbon (WSOC) in South Asian aerosols. Journal of Geophysical Research: Atmospheres 2013; 118: 614-626.

Kirillova EN, Andersson A, Tiwari S, Srivastava AK, Bisht DS, Gustafsson Ö. Water-soluble organic carbon aerosols during a full New Delhi winter: Isotope-based source apportionment and optical properties. Journal of Geophysical Research: Atmospheres 2014b; 119: 3476-3485.

Krishnaswami S, Singh SK. Silicate and carbonate weathering in the drainage basins of the Ganga-Ghaghara-Indus head waters: Contributions to major ion and Sr isotope geochemistry. Proceedings of the Indian Academy of Sciences-Earth and Planetary Sciences 1998; 107: 283-291.

Kroll JH, Seinfeld JH. Chemistry of secondary organic aerosol: Formation and evolution of low-volatility organics in the atmosphere. Atmospheric Environment 2008; 42: 3593-3624.

Kumar A, Sarin MM, Sudheer AK. Mineral and anthropogenic aerosols in Arabian Sea–atmospheric boundary layer: Sources and spatial variability. Atmospheric Environment 2008a; 42: 5169-5181.

Kumar A, Sudheer A, Sarin M. Chemical characteristics of aerosols in MABL of Bay of Bengal and Arabian Sea during spring inter-monsoon: a comparative study. Journal of Earth System Science 2008b; 117: 325-332.

Kumar SP, Ramaiah N, Gauns M, Sarma VVSS, Muraleedharan PM, Raghukumar S, et al. Physical forcing of biological productivity in the Northern Arabian Sea during the Northeast Monsoon. Deep Sea Research Part II: Topical Studies in Oceanography 2001; 48: 1115-1126.

Kundu S, Kawamura K, Andreae TW, Hoffer A, Andreae MO. Diurnal variation in the water-soluble inorganic ions, organic carbon and isotopic compositions of total carbon and nitrogen in biomass burning aerosols from the LBA-SMOCC campaign in Rondônia, Brazil. Journal of Aerosol Science 2010a; 41: 118-133.

Kundu S, Kawamura K, Lee M. Seasonal variation of the concentrations of nitrogenous species and their nitrogen isotopic ratios in aerosols at Gosan, Jeju Island: Implications for atmospheric processing and source changes of aerosols. Journal of Geophysical Research: Atmospheres 2010b; 115.

Kunwar B, Torii K, Zhu C, Fu P, Kawamura K. Springtime variations of organic and inorganic constituents in submicron aerosols (PM1.0) from Cape Hedo, Okinawa. Atmospheric Environment 2016; 130: 84-94.

Lelieveld J, Crutzen PJ, Ramanathan V, Andreae MO, Brenninkmeijer CAM, Campos T, et al. The Indian Ocean Experiment: Widespread Air Pollution from South and Southeast Asia. Science 2001; 291: 1031-1036.

Li Y, Pöschl U, Shiraiwa M. Molecular corridors and parameterizations of volatility in the chemical evolution of organic aerosols. Atmos. Chem. Phys. 2016; 16: 3327-3344.

López-Veneroni D. The stable carbon isotope composition of PM2. 5 and PM10 in Mexico City Metropolitan Area air. Atmospheric Environment 2009; 43: 4491-4502.

Madhupratap M, Kumar SP, Bhattathiri PMA, Kumar MD, Raghukumar S, Nair KKC, et al. Mechanism of the biological response to winter cooling in the northeastern Arabian Sea. Nature 1996; 384: 549-552.

Mamane Y, Gottlieb J. Nitrate formation on sea-salt and mineral particles—A single particle approach. Atmospheric Environment. Part A. General Topics 1992; 26: 1763-1769.

Martinelli LA, Camargo PB, Lara LBLS, Victoria RL, Artaxo P. Stable carbon and nitrogen isotopic composition of bulk aerosol particles in a C4 plant landscape of southeast Brazil. Atmospheric Environment 2002; 36: 2427-2432.

Miyazaki Y, Kawamura K, Jung J, Furutani H, Uematsu M. Latitudinal distributions of organic nitrogen and organic carbon in marine aerosols over the western North Pacific. Atmospheric Chemistry and Physics 2011; 11: 3037-3049.

Morera-Gómez Y, Cong Z, Widory D. Carbonaceous Fractions Contents and Carbon Stable Isotope Compositions of Aerosols Collected in the Atmosphere of Montreal (Canada): Seasonality, Sources, and Implications. Frontiers in Environmental Science 2021; 9.

Morera-Gómez Y, Santamaría JM, Elustondo D, Alonso-Hernández CM, Widory D. Carbon and nitrogen isotopes unravels sources of aerosol contamination at Caribbean rural and urban coastal sites. Science of The Total Environment 2018; 642: 723-732.

Naqvi S. Some aspects of the oxygen-deficient conditions and denitrification in the Arabian Sea. Journal of Marine research 1987; 45: 1049-1072.

Naqvi W. Geographical extent of denitrification in the Arabian Sea in relation to some physical processes. Oceanologica Acta 1991; 14: 281-290.

Pani SK, Lee C-T, Chou CCK, Shimada K, Hatakeyama S, Takami A, et al. Chemical Characterization of Wintertime Aerosols over Islands and Mountains in East Asia: Impacts of the Continental Asian Outflow. Aerosol and Air Quality Research 2017; 17: 3006-3036.

Park Y-m, Park K-s, Kim H, Yu S-m, Noh S, Kim M-s, et al. Characterizing isotopic compositions of TC-C, NO3−-N, and NH4+-N in PM2.5 in South Korea: Impact of China's winter heating. Environmental Pollution 2018; 233: 735-744.

Parnell A. Simmr: a stable isotope mixing model. R package version 0.4.1. 2020.

Pavuluri CM, Kawamura K. Evidence for 13-carbon enrichment in oxalic acid via iron catalyzed photolysis in aqueous phase. Geophysical Research Letters 2012; 39: doi:10.1029/2011GL050398.

Pavuluri CM, Kawamura K. Enrichment of 13C in diacids and related compounds during photochemical processing of aqueous aerosols: New proxy for organic aerosols aging. Scientific Reports 2016; 6: 36467.

Pavuluri CM, Kawamura K, Tachibana E, Swaminathan T. Elevated nitrogen isotope ratios of tropical Indian aerosols from Chennai: Implication for the origins of aerosol nitrogen in South and Southeast Asia. Atmospheric Environment 2010; 44: 3597-3604.

Pease PP, Tchakerian VP, Tindale NW. Aerosols over the Arabian Sea: geochemistry and source areas for aeolian desert dust. Journal of Arid Environments 1998; 39: 477-496.

Prospero JM, Ginoux P, Torres O, Nicholson SE, Gill TE. Environmental characterization of global sources of atmospheric soil dust identified with the Nimbus 7 Total Ozone Mapping Spectrometer (TOMS) absorbing aerosol product. Reviews of geophysics 2002; 40.

Qu Z, Henze DK, Worden HM, Jiang Z, Gaubert B, Theys N, et al. Sector-based top-down estimates of NOx, SO2, and CO emissions in East Asia. Geophysical Research Letters 2022: e2021GL096009.

Ram K, Sarin M, Tripathi S. A 1 year record of carbonaceous aerosols from an urban site in the Indo-Gangetic Plain: characterization, sources, and temporal variability. Journal of Geophysical Research: Atmospheres (1984–2012) 2010; 115: doi: 10.1029/2010JD014188.

Rastogi N, Agnihotri R, Sawlani R, Patel A, Babu SS, Satish R. Chemical and isotopic characteristics of PM10 over the Bay of Bengal: Effects of continental outflow on a marine environment. Science of The Total Environment 2020; 726: 138438.

Rastogi N, Sarin MM. Chemistry of aerosols over a semi-arid region: Evidence for acid neutralization by mineral dust. Geophysical Research Letters 2006; 33.

Sarin M, Krishnaswami S, Dilli K, Somayajulu B, Moore W. Major ion chemistry of the Ganga-Brahmaputra river system: weathering processes and fluxes to the Bay of Bengal. Geochimica et cosmochimica acta 1989; 53: 997-1009.

Sarin M, Krishnaswami S, Trivedi J, Sharma K. Major ion chemistry of the Ganga source waters: weathering in the high altitude Himalaya. Proceedings of the Indian Academy of Sciences-Earth and Planetary Sciences 1992; 101: 89-98.

Schlitzer R. Interactive analysis and visualization of geoscience data with Ocean Data View. Computers & geosciences 2002; 28: 1211-1218.

Sharma S, Mandal T, Shenoy D, Bardhan P, Srivastava MK, Chatterjee A, et al. Variation of stable carbon and nitrogen isotopic composition of PM 10 at urban sites of Indo Gangetic Plain (IGP) of India. Bulletin of environmental contamination and toxicology 2015; 95: 661-669.

Sheesley RJ, Kirillova E, Andersson A, Kruså M, Praveen P, Budhavant K, et al. Year-round radiocarbon-based source apportionment of carbonaceous aerosols at two background sites in South Asia. Journal of Geophysical Research: Atmospheres (1984–2012) 2012; 117.

Singh GK, Choudhary V, Rajeev P, Paul D, Gupta T. Understanding the origin of carbonaceous aerosols during periods of extensive biomass burning in northern India. Environmental Pollution 2021a; 270: 116082.

Singh GK, Paul D, Rajput P, Gupta T. Stable Carbon Isotope and Bulk Composition of Wintertime Aerosols from Kanpur. In: Gupta T, Agarwal AK, Agarwal RA, Labhsetwar NK, editors. Environmental Contaminants: Measurement, Modelling and Control. Springer Singapore, Singapore, 2018, pp. 209-220.

Singh GK, Rajeev P, Paul D, Gupta T. Chemical characterization and stable nitrogen isotope composition of nitrogenous component of ambient aerosols from Kanpur in the Indo-Gangetic Plains. Science of The Total Environment 2021b; 763: 143032.

Stein A, Draxler R, Rolph G, Stunder B, Cohen M, Ngan F. NOAA's HYSPLIT atmospheric transport and dispersion modeling system. Bulletin of the American Meteorological Society 2015; 96: 2059-2077.

Still C, Berry J, Collatz G, DeFries R, Hall F, Meeson B, et al. ISLSCP II C4 vegetation percentage. ORNL DAAC 2009.

Tindale NW, Pease PP. Aerosols over the Arabian Sea: Atmospheric transport pathways and concentrations of dust and sea salt. Deep Sea Research Part II: Topical Studies in Oceanography 1999; 46: 1577-1595.

Turekian VC, Macko S, Ballentine D, Swap RJ, Garstang M. Causes of bulk carbon and nitrogen isotopic fractionations in the products of vegetation burns: laboratory studies. Chemical Geology 1998; 152: 181-192.

Vodička P, Kawamura K, Schwarz J, Kunwar B, Ždímal V. Seasonal study of stable carbon and nitrogen isotopic composition in fine aerosols at a Central European rural background station. Atmos. Chem. Phys. 2019; 19: 3463-3479.

Ward BB, Devol AH, Rich JJ, Chang BX, Bulow SE, Naik H, et al. Denitrification as the dominant nitrogen loss process in the Arabian Sea. Nature 2009; 461: 78-81.

Widory D. Combustibles, fuels and their combustion products: A view through carbon isotopes. Combustion Theory and Modelling 2006; 10: 831-841.

Widory D. Nitrogen isotopes: Tracers of origin and processes affecting PM10 in the atmosphere of Paris. Atmospheric Environment 2007; 41: 2382-2390.

Wu P-M, Okada K. Nature of coarse nitrate particles in the atmosphere—A single particle approach. Atmospheric Environment 1994; 28: 2053-2060.

Xiao H-W, Xiao H-Y, Luo L, Zhang Z-Y, Huang Q-W, Sun Q-B, et al. Stable carbon and nitrogen isotope compositions of bulk aerosol samples over the South China Sea. Atmospheric Environment 2018; 193: 1-10.

Zhang Y-L, Li J, Zhang G, Zotter P, Huang R-J, Tang J-H, et al. Radiocarbon-Based Source Apportionment of Carbonaceous Aerosols at a Regional Background Site on Hainan Island, South China. Environmental Science & Technology 2014; 48: 2651-2659.

Zhang YL, Huang RJ, El Haddad I, Ho KF, Cao JJ, Han Y, et al. Fossil vs. non-fossil sources of fine carbonaceous aerosols in four Chinese cities during the extreme winter haze episode of 2013. Atmos. Chem. Phys. 2015; 15: 1299-1312.

Zheng L, Yang X, Lai S, Ren H, Yue S, Zhang Y, et al. Impacts of springtime biomass burning in the northern Southeast Asia on marine organic aerosols over the Gulf of Tonkin, China. Environmental Pollution 2018; 237: 285-297.

Table 1. Stable carbon and nitrogen isotopic composition of TC and TN, respectively, in TSP samples collected over the Arabian Sea during winter cruise (6-24 December 2018).

id	TC (μg m^{-3})	TN (μg m^{-3})	$\delta^{13}C_{TC}$ (‰)	$\delta^{13}C_{TC\text{-}remained}$ (‰)*	$\delta^{15}N_{TN}$(‰)
SS379#1	3.1	0.9	-24.5	-26.1	16.9
SS379#2	5.1	2.2	-24.6	-25.1	18.5
SS379#3	8.5	4.8	-25.1	-25.4	15.3
SS379#4	5.5	2.2	-24.1	-24.5	22.4
SS379#5	5.7	2.0	-24.4	-24.8	25.1
SS379#6	4.2	1.9	-24.0	-24.7	22.8
SS379#7	4.9	2.6	-24.7	-25.3	16.6
SS379#8	5.8	1.8	-23.7	-23.9	22.8
SS379#9	8.4	3.5	-23.9	-24.0	20.2
SS379#10	13.4	5.0	-23.0	-23.2	16.5
SS379#11	9.0	2.6	-22.9	-23.0	21.1
SS379#12	8.0	2.0	-23.9	-24.1	19.4
SS379#13	6.0	1.9	-23.0	-23.5	15.8
SS379#14	7.0	2.9	-23.6	-23.9	17.0
SS379#15	2.1	3.6	-24.2	-24.4	19.6
SS379#16	13.3	3.5	-25.1	-24.8	19.5
SS379#17	12.4	5.0	-24.1	-25.1	22.7

Note: *Aerosol filter punches are exposed to HCl fumes in a desiccator for 6 h.

Table 2. Comparison of mass concentrations (μg m^{-3}) of TC and TN along with their stable carbon isotopic composition ($\delta^{13}C_{TC}$), and nitrogen iosotopic composition ($\delta^{15}N_{TN}$) over the world's oceans around the globe.

Region	Type	Duration	TC (μg m^{-3})	TN (μg m^{-3})	TC/TN	$\delta^{13}C_{TC}$ (‰)	$\delta^{15}N_{TN}$ (‰)	Reference
Arabian Sea	TSP	6-28 Dec'18	2.1 -13.4 (7.2)	0.9 - 5.0 (2.8)	0.6 - 4.0 (2.7)	-25.1 to -22.9 (-23.4)	+15.3 to +25.1 (+19.5)	This study
Arabian Sea	TSP	19 Mar- 12 April' 06	24-71 (35)	0.5 -1.2 (0.7)	34 - 65 (50)	-27.5 to -24.3 (-26.5)	-2.3 to +12.7 (+1.1)	Agnihotri et al., 2012
Bay of Bengal (IGP-outflow)	$PM_{2.5}$	27 Dec'08 - 26 Jan'09	3.6-15.4 (8.1)	0.6-8.8 (3.7)	1.3 - 9.4 (3.0)	-25.0 to -22.8 (-23.8)	+11.8 to +30.6 (+20.4)	Bikkina et al., 2016
Bay of Bengal (SEA-outflow)	$PM_{2.5}$	27 Dec'08 - 26 Jan'09	1.1-6.5 (3.8)	0.2-3.0 (1.4)	1.9 -5.4 (2.9)	-26.9 to -24.2 (-25.3)	+10.4 to +31.7 (+19.4)	Bikkina et al., 2016
Bay of Bengal	TSP	18 April- 8 May'06	1.0 - 45.1 (8.4)	0.6 - 3.3 (1.8)	0.7 - 37.6 (6.9)	-26.6 to -24.1 (-25.6)	+6.4 to +15.2 (+10.6)	Agnihotri et al., 2012
East China Sea	TSP	Oct-Nov'15	5.04 ± 3.08	0.93 ± 0.59		−22.9 ± 1.7	+0.7 ± 3.3	Xiao et al., 2017
Baltic Sea		9-17 Nov'12				–26.4	–0.2 to 0.8	Garbarienė et al. 2015
Western North Pacific	TSP	24 Aug - 13 Sept'08				-22.1 to -20.8 (-21.0)	-2.2 to +8.9 (+4.9)	Miyazaki et al., 2011
Nainital, India	TSP	Sept'06 – Jun'07	5.3 -11 (7.9)	0.35-1.3 (0.77)		-25 to -23 (-24)	+22 to +26 (+24)	Hegde et al., 2016
Delhi, India	$PM_{2.5}$	Oct'-Nov'16	9.5-486 (197)	0.7-90.7 (27.8)	5.3 - 130 (28.8)	-25.4 to -27.0 (-26.4)	+12.5 to +30.9 (+16.9)	Salvani et al., 2019
Delhi, India	PM_{10}	Jan – Dec'11	13.1 - 125.9 (53.0)	1.5 - 42.6 (14.9)	4.8-20.2 (9.8)	-26.4 to -24.8 (–25.5)	+3.3 to +14.3 (+9.6)	Sharma et al., 2015
Varanasi, India	PM_{10}	Jan – Dec'11	9.3 - 51.9 (27.1)	2.3 - 36.6 (9.8)	2.1-16.3 (9.2)	-26.4 to -23.3 (–25.4)	+2.8 to +11.0 (+6.8)	Sharma et al., 2015
Kolkata, India	PM_{10}	Jan – Dec'11	9.1 - 98.2 (32.6)	1.4 - 25.9 (9.3)	4.4-25.9 (11)	-26.6 to -24.9 (–26.0)	+2.8 to +11.5 (+7.4)	Sharma et al., 2015
Chennai, India	TSP	Winter 2007	10-66	2.1-72		-25.7 to -24.0 (-24.5)	+18.1 to +24.5 (21.2)	Pavuluri et al., 2012
Mumbai, India	PM10	13-18 Feb'2007	22±4.7	2.4±1.3		-25.9±0.3	+21.3±1.8	Aggarwal et al., 2015
Goa, India		Dec'09 – Jan'11	26.3±9.4	5.6±2.8	6.0±1.5	-24.8±0.9	10.8±2.2	Agnihotri et al., 2015
Guangzhou, China	TSP	Oct-Nov'15	19.27 ± 10.11	6.44 ± 4.34		−25.8 ± 0.4	+13.2 ± 0.9	Xiao et al., 2017
Gosan, S.Korea	TSP	Mar-June'07, 16-24 April'18	12-19 (16)	4.8-11(7.7)	1.2–3.9(2.5)	-23.3 to -20.4 (-21.8)		Jung & Kawamura, 2011
Thailand forest fires	PM2.5	Mar-April'15	1.4 -80 (34)	0.7-8.6 (3.0)		-23.8 to -29.8 (-26.0)	+15.8 to +25.1 (19.4)	Boreddy et al., 2018
Okinawa, Japan			2.0±0.6	1.2±0.6	1.9±0.7	-22.5±0.6	+13.6±1.7	Kunwar et al., 2012
South China Sea		Cool season	5.0±3.1	0.93±0.59		-22.9±1.7	+0.7±3.3	Xiao et al., 2018

Here, IGP= Indo-Gangetic Plain and SEA: Southeast Asia

Table 3. Stable carbon isotopic composition of particles from the source-emissions.

Source	Parameter	$\delta^{13}C_{TC}$(‰)	Reference
Biomass burning emissions			
Thailand (mostly C3)	TC	-26.0±1.2	(Boreddy et al., 2018)
Santarem, Brazil (mostly C3)	TC	-25.8±0.52	(Martinelli et al., 2002)
Rondonia, Brazil (mostly C3)	TC	-25.5	(Kundu et al., 2010a)
Punjab, India (mostly C3)	TC	-26.6	(Singh et al., 2021a)
Sao Paulo, Brazil (C4)	TC	-20.9±0.75	(Martinelli et al., 2002)
Straw Pellets	TC	-28.4±0.2	(Garbaras et al., 2015)
Wood burning emissions			
New Zealand	TC	-24.9 to -27.6	(Ancelet et al., 2013)
India	TC	-28.4±0.9	((Agnihotri et al., 2011a))
Laboratory combustions	TC	-26.0±0.1	(Garbaras et al., 2015)
vehicular emissions			
Zhujian tunnel, China	TC	-25.0±0.3	(Dai et al., 2015)
Mount Victoria tunnel, New Zealand	TC	-25.9±0.8	(Ancelet et al., 2011)
tunnel of Avenida Chapultepec, Mexico	TC	-25.5±0.1	(López-Veneroni, 2009)
Road traffic emissions, Delhi, India	TC	-25.3	(Agnihotri et al., 2011a)
Car tailpipe (Diesel)	TC	-26.3	(Morera-Gómez et al., 2018)
Car tailpipe (Gasoline)	TC	-25.2	(Morera-Gómez et al., 2018)
Coal combustion			
Paris	TC	-23.9±0.5	(Widory, 2006)
Australia	TC	-25.5±0.8	(Feng et al., 2020)
Russia	TC	-23.22±1.2	(Feng et al., 2020)
India	TC	-22.4±0.1	(Agnihotri et al., 2020)
Dust			
India, surface soil	TC	-10.5±4.0	(Agnihotri et al., 2020)
Steet dust, Mexico	TC	-21±0.2	(López-Veneroni, 2009)
Asian dust	TC	-1.6,-9.8	(López-Veneroni, 2009)
Road dust	TC	-13.1±2.0	(Morera-Gómez et al., 2018)
Top soil	TC	-20.5±4.8	(Morera-Gómez et al., 2018)
Marine Organic matter			
North Pacific	TC	-21±1.9	(Miyazaki et al., 2011)
Amsterdam island	TC	-21.6±0.6	(Cachier et al., 1986)

Table 4. Stable carbon isotopic composition of particles from the source-emissions.

Biomass burning	**Parameter**	**$\delta^{15}N_{TN}$(‰)**	**Reference**
Thailand (mostly C3)	TN	19.4±2.1	(Boreddy et al., 2018)
Rondonia, Brazil	TN	23.3±1.7 (day) 23.7±1.4 (night)	(Kundu et al., 2010a)
India (mostly C3)	TN	10.4 ± 5.7	(Agnihotri et al., 2011a)
Sao Paulo, Brazil (C4 & pasture site)	TN	7-18.7 (10.6±2.8)	(Martinelli et al., 2002)
Wood burning emissions			
India	TN	15.4±2.9	(Agnihotri et al., 2011a)
vehicular emissions			
Paris	TN	4.6±0.6	(Widory, 2007)
Car tailpipe (Diesel)	TN	1.6	(Morera-Gómez et al., 2018)
Car tailpipe (Gasoline)	TN	1.2	(Morera-Gómez et al., 2018)
Coal combustion			
India	TN	8.7, 7.1	(Agnihotri et al., 2011a)
Dust			
Thar, Rajastha, India	TN	-10.5±4.0	(Agnihotri et al., 2020)
Asian dust	TN	2.5, 2.7	(Kawamura et al., 2004)

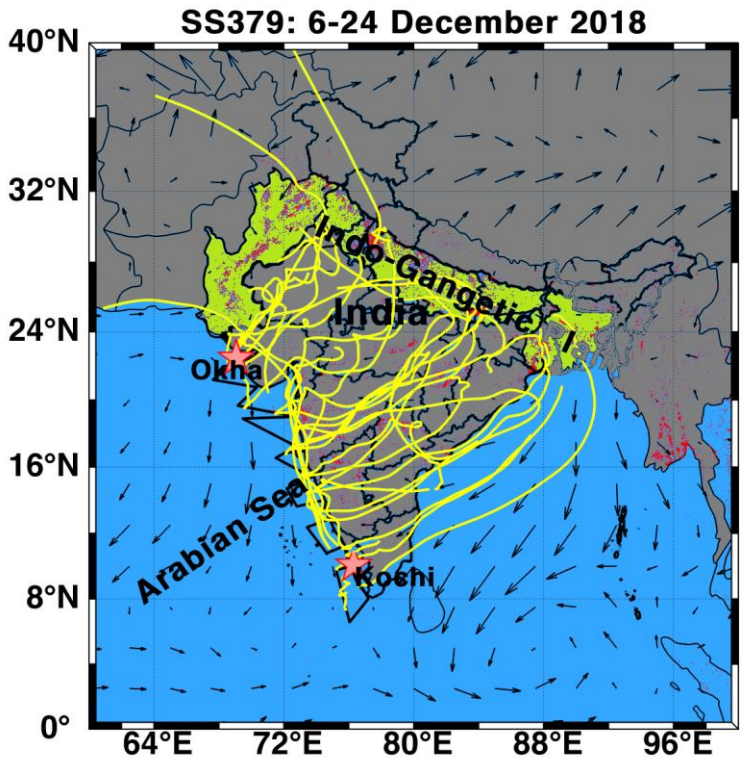

Figure 1. Cruise track and backward air mass trajectories of TSP collected over the Arabian Sea during SS379 cruise (6-28 December 2018). The dashed black lines represent the 100 m asl backward air mass trajectories computed using NOAA Hybrid Single Particle Lagrangian Integrated Trajectory Model (HYSPLIT) for the sampling days. The red dots on the continent is the fire counts retrieved from the moderate resolution imaging spectroradiometer (MODIS) satellite.

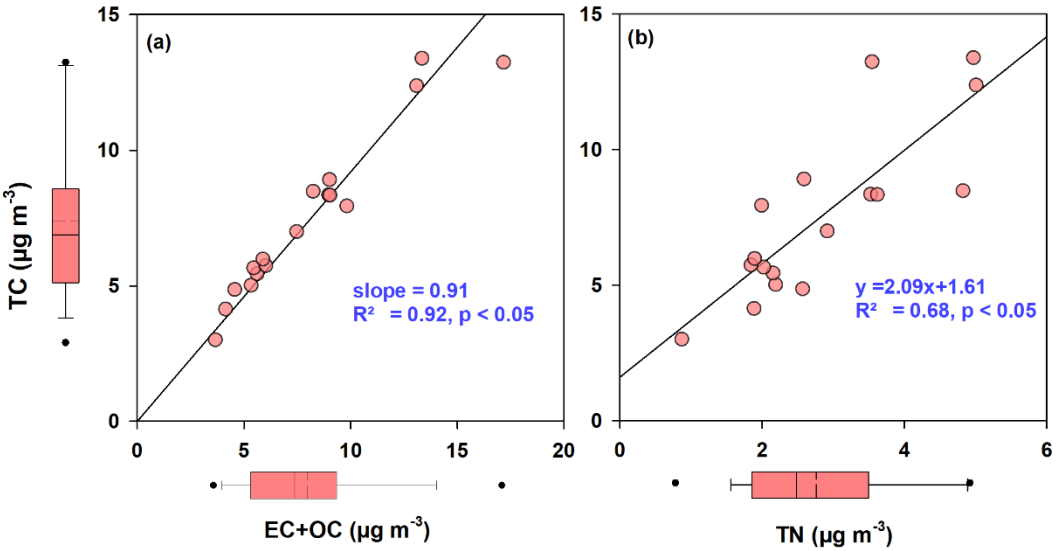

Figure 2. Linear regression analysis between the concentrations of total carbon (TC) versus (a) sum of elemental carbon (EC) and organic carbon (OC) and (b) total nitrogen (TN) in the TSP samples collected over the Arabian Sea during SS379 cruise (6-24 December 2018). The whiskers (5 and 95 percentile), edges (25 and 75 percentile), the solid (50 percentile) and dashed lines (mean) in the box plots represent the overall distribution of concentrations of TC and TN.

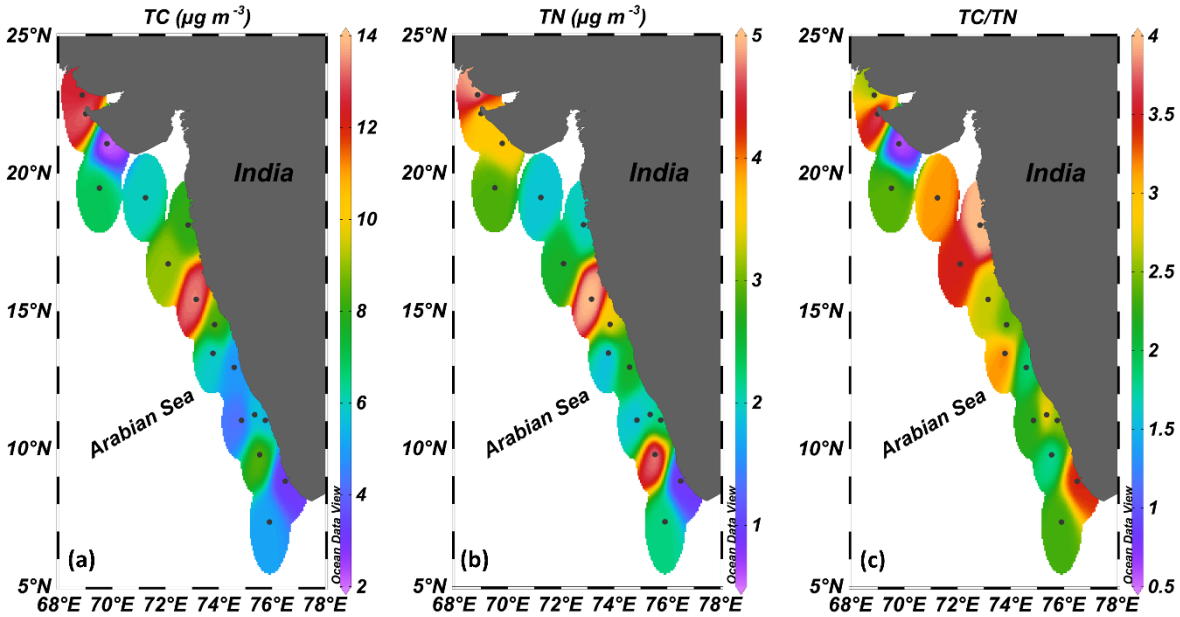

Figure 3. Spatial variability of concentrations of (a) total carbon (TC), (b) total nitrogen (TN), (c) TC/TN ratios in TSP samples collected over Arabian Sea during SS379 cruise (6-28 December 2018). The spatial contours were generated through the interpolation techniques in the Ocean Data View software (Schlitzer, 2002).

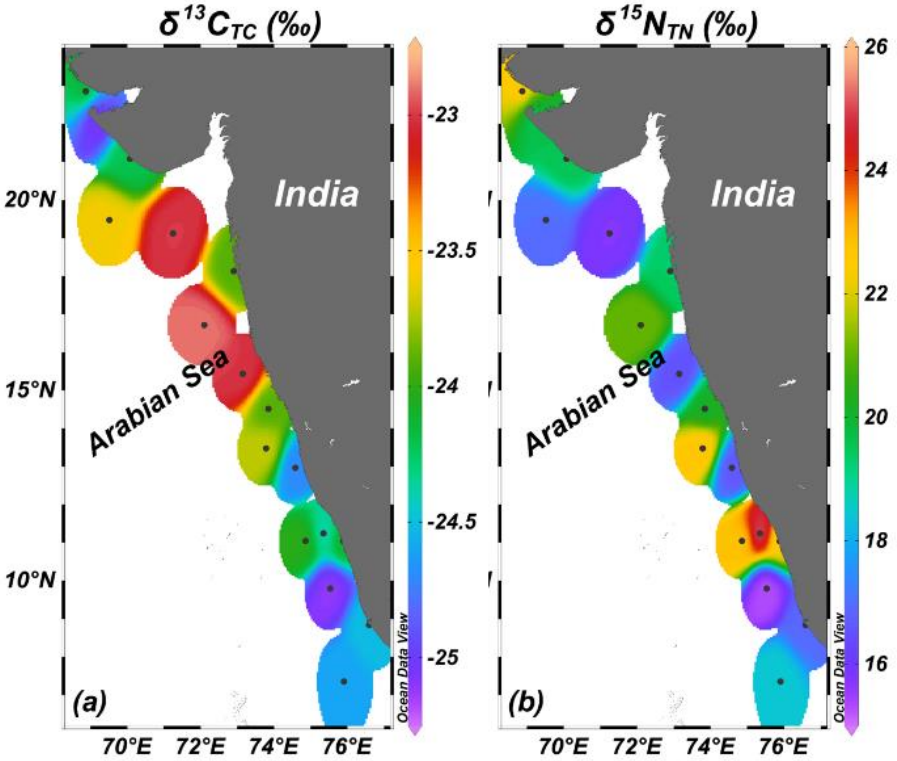

Figure 4. Spatial variability of (a) stable carbon isotopic composition of TC ($\delta^{13}C_{TC}$), and (b) nitrogen isotopic composition of TN ($\delta^{15}N_{TN}$) in marine aerosols collected over the Arabian Sea.

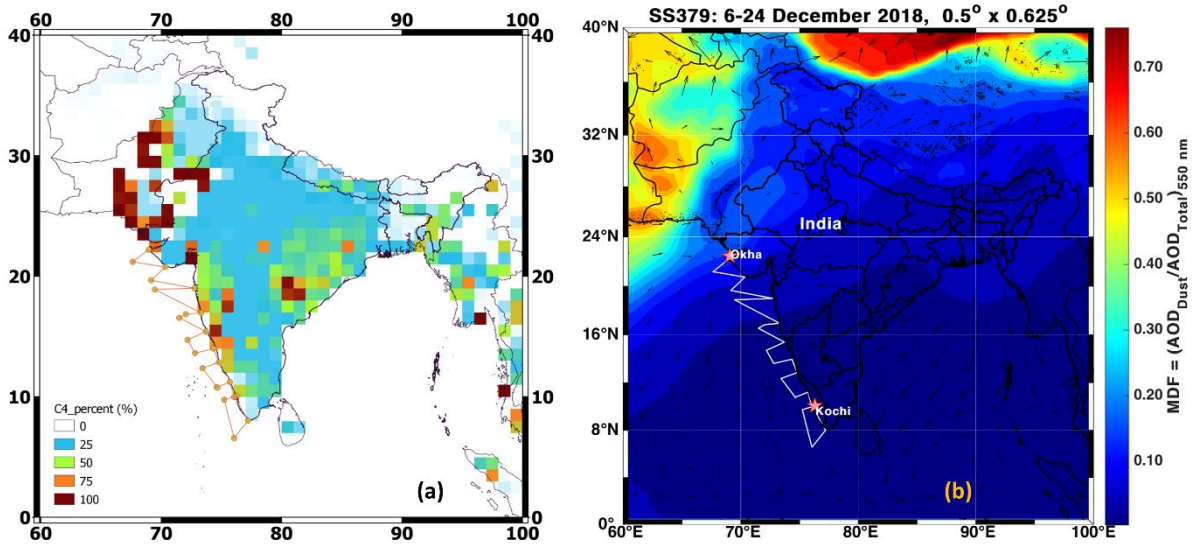

Figure 5. (a) Geograpahically spanned projection of C_4 vegetation over South Asia adopted from Still et al. (2009) along with the cruise track of SS379 and (b) MERRA-simulations based mineral dust fraction (MDF), which is the ratio of aerosol optical depth caused by the dust (AOD_{dust}) to total columnar particles (AOD_{total}).

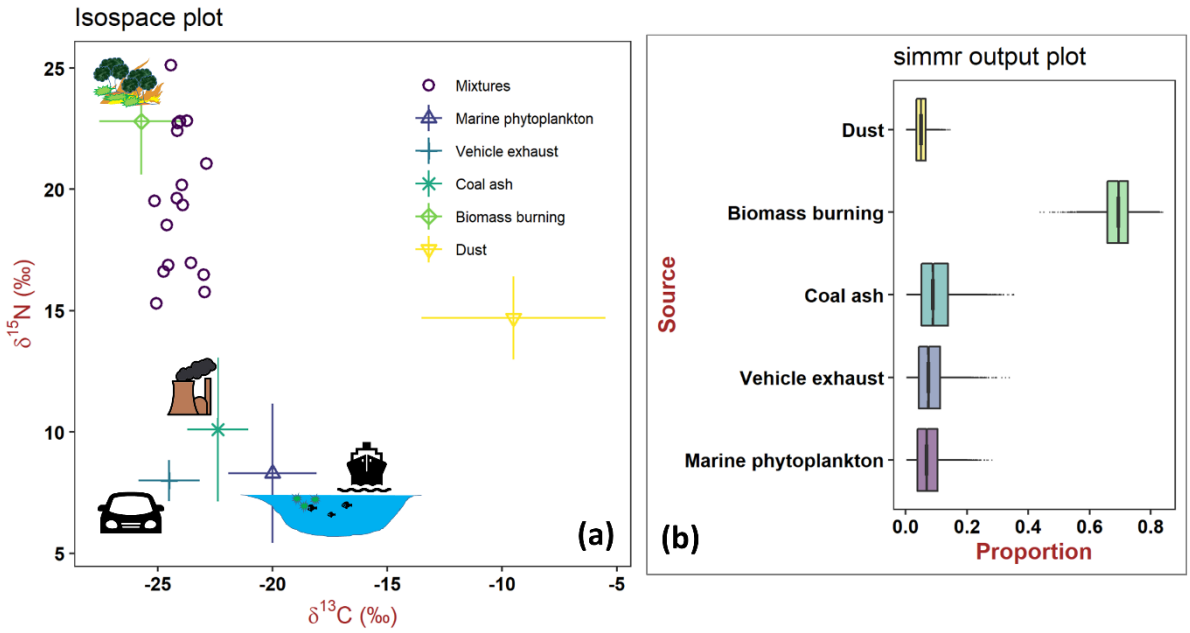

Figure 6. Dual isotope isospace plot of $\delta^{13}C$ versus $\delta^{15}N$ of TC and TN in marine aerosols from the Arabian Sea along with source-emission endmembers, (b) overall individual source emission contributions over the Arabian Sea using Bayesian isotope mixing model.

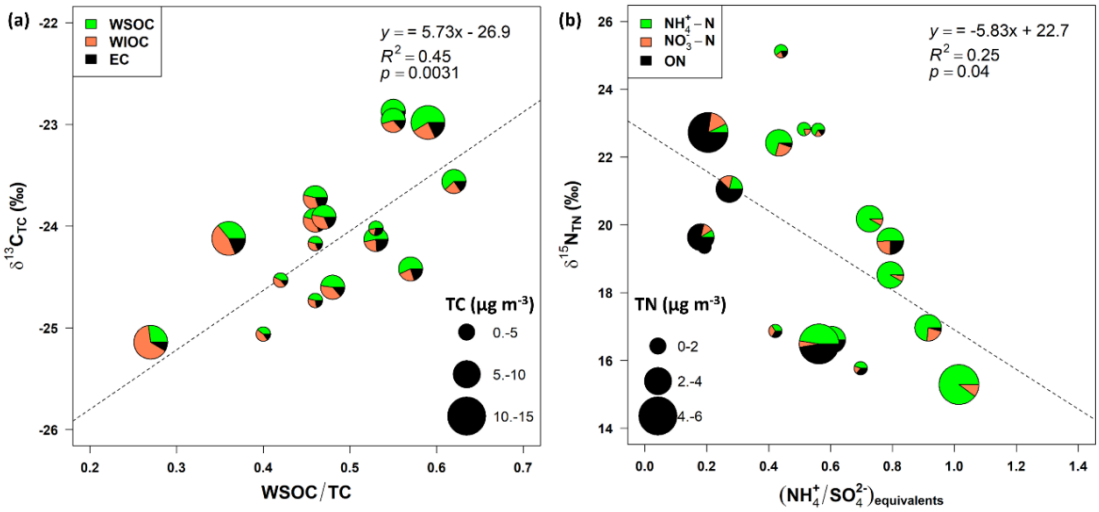

Figure 7. Linear regression analyses between (a) $\delta^{13}C_{TC}$ (‰) and mass ratio of WSOC/TC with the information of TC concentrations (*i.e.*, symbol size) and carbonaceous component fractions (piechart), and (b) $\delta^{15}N_{TN}$ (‰) and equivalent ratio of NH_4^+/nss-SO_4^{2-} with the information of TN concentrations (symbol size) and constituent nitrogen fractions (piechart) in marine aerosols collected from the Arabian Sea cruise (6-24 December 2018). Here, Pearson's critical-r value with 15 degrees of freedom is 0.48 at the 0.05 is the level of significance.

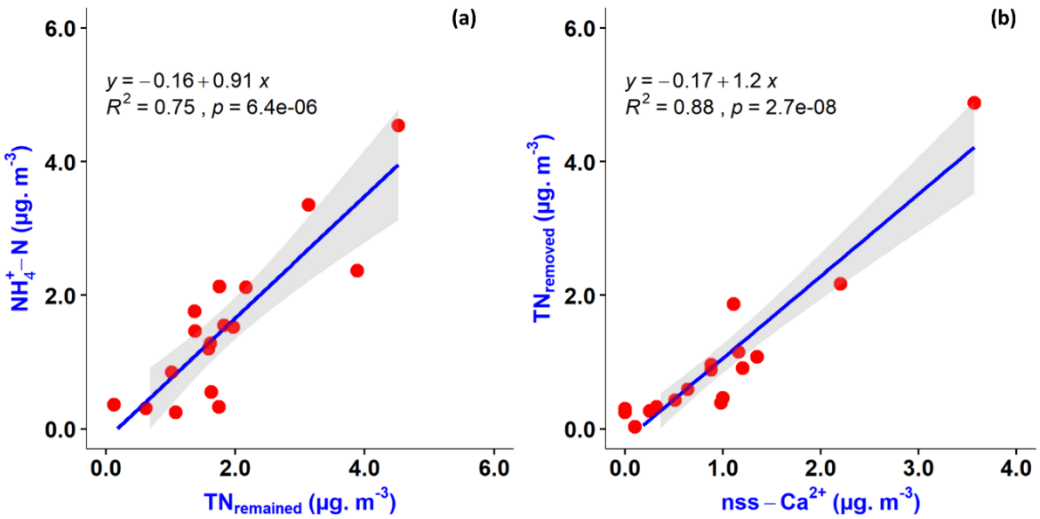

Figure 8. Linear regression analyses for mass concentrations between (a) NH_4^+-N and $TN_{remained}$, (b) $TN_{removed}$ and nss-Ca^{2+} in marine aerosols collected during the Arabian Sea cruise. For the definition of terms, please see the text.

[Science of the Total Environment]

Supporting Information for

Unraveling the sources of atmospheric organic aerosols over the Arabian Sea: insights from the stable carbon and nitrogen isotopic composition

By

Poonam Bikkina[1,*], Srinivas Bikkina[1,2], Kimitaka Kawamura[2], V.V.S.S. Sarma[3], Dhananjay K. Deshmukh[2]

[1]CSIR-National Institute of Oceanography, Dona Paula, Goa 403 004, India
[2]Chubu Institute of Advanced Sciences, Chubu University, Kasugai-shi, Aichi, 4878501, Japan
[3]CSIR-National Institute of Oceanography, Regional Cente Waltair, Visakhapatnam 530017, India

Contents of this file

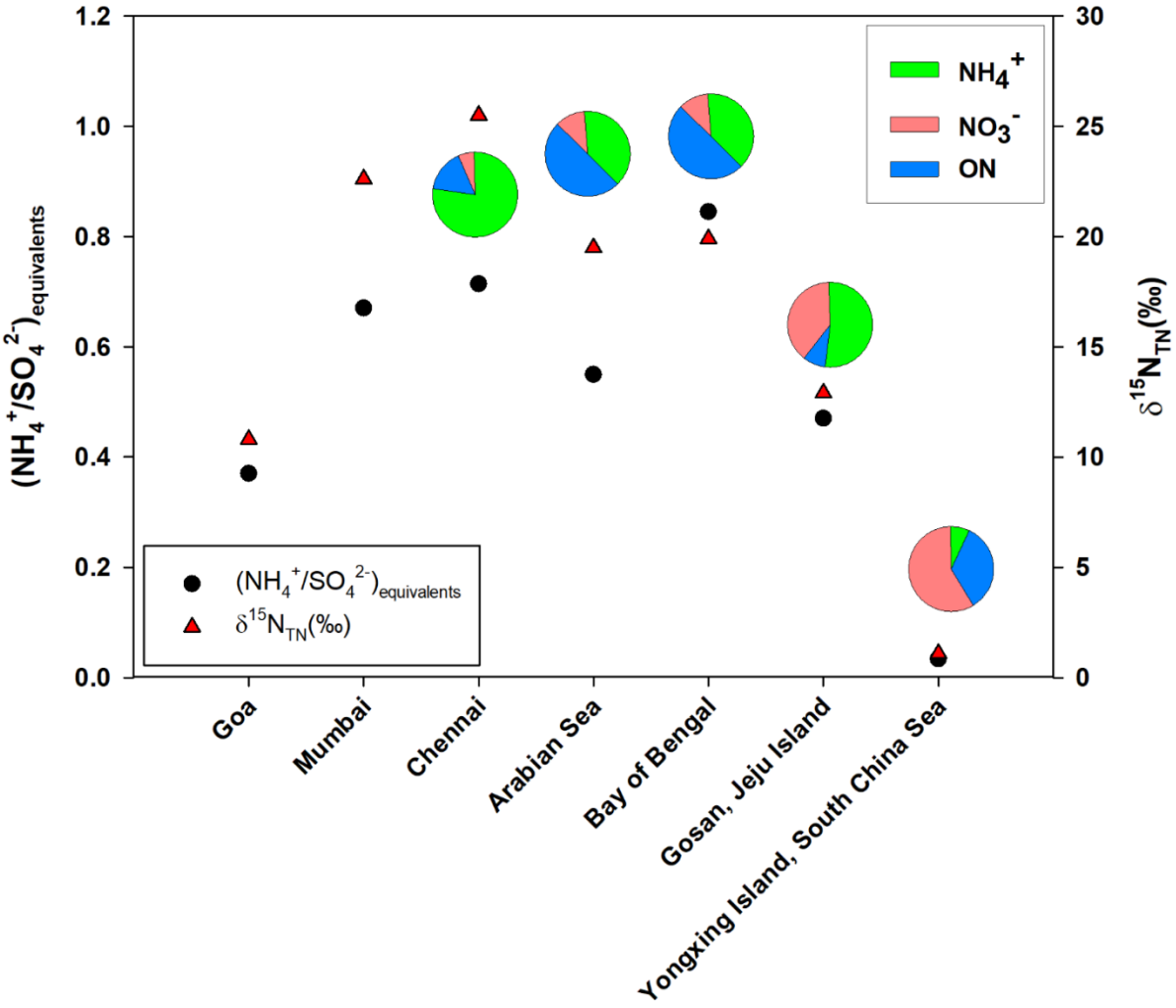

Figure S1. Scatter plot between South Asia and East Asia for $\delta^{15}N_{TN}$ vs. NH_4^+/SO_4^{2-}